Nucleic Acids Research, 2025, **53**, gkaf136
https://doi.org/10.1093/nar/gkaf136
NAR Breakthrough Article

A new level of RNA-based plant protection: dsRNAs designed from functionally characterized siRNAs highly effective against *Cucumber mosaic virus*

Marie Knoblich[1,†], Torsten Gursinsky[1,†], Selma Gago-Zachert[1], Claus Weinholdt[2], Jan Grau[2], Sven-Erik Behrens[1,*]

[1]Institute of Biochemistry and Biotechnology, Martin Luther University Halle-Wittenberg, Charles Tanford Protein Centre, Kurt-Mothes-Str. 3A, 06120 Halle (Saale), Germany
[2]Institute of Computer Science, Martin Luther University Halle-Wittenberg, Von-Seckendorff-Platz 1, 06120 Halle (Saale), Germany

[*]To whom correspondence should be addressed. Email: sven.behrens@biochemtech.uni-halle.de
[†]The first two authors should be regarded as Joint First Authors.

Abstract

RNA-mediated crop protection increasingly becomes a viable alternative to agrochemicals that threaten biodiversity and human health. Pathogen-derived double-stranded RNAs (dsRNAs) are processed into small interfering RNAs (siRNAs), which can then induce silencing of target RNAs, e.g. viral genomes. However, with currently used dsRNAs, which largely consist of undefined regions of the target RNAs, silencing is often ineffective: processing in the plant generates siRNA pools that contain only a few functionally effective siRNAs (*e*siRNAs). Using an *in vitro* screen that reliably identifies *e*siRNAs from siRNA pools, we identified *e*siRNAs against *Cucumber mosaic virus* (CMV), a devastating plant pathogen. Topical application of *e*siRNAs to plants resulted in highly effective protection against massive CMV infection. However, optimal protection was achieved with newly designed multivalent 'effective dsRNAs' (*e*dsRNAs), which contain the sequences of several *e*siRNAs and are preferentially processed into these *e*siRNAs. The *e*siRNA components can attack one or more target RNAs at different sites, be active in different silencing complexes, and provide cross-protection against different viral variants—important properties for combating rapidly mutating pathogens such as CMV. *e*siRNAs and *e*dsRNAs have thus been established as a new class of 'RNA actives' that significantly increase the efficacy and specificity of RNA-mediated plant protection.

Graphical abstract

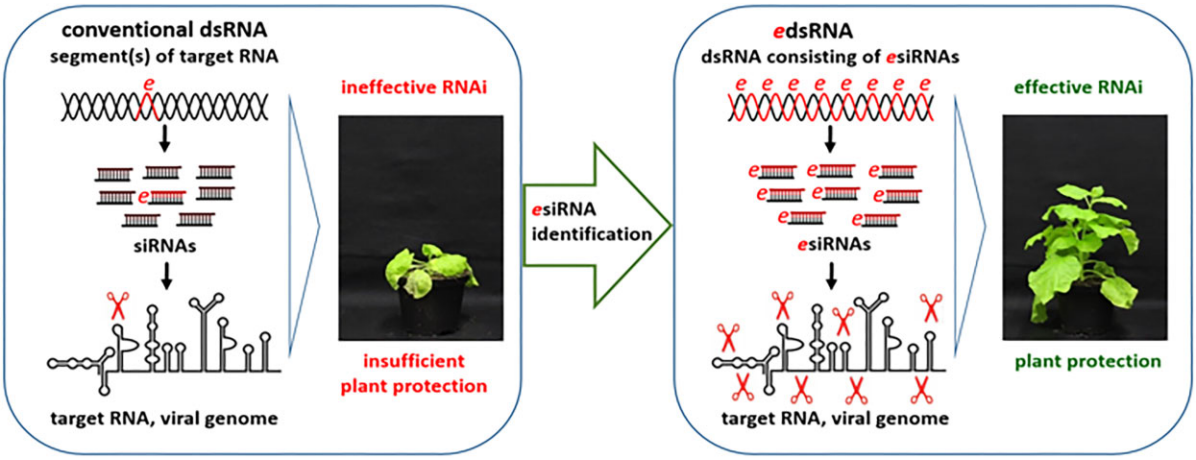

Introduction

Virus-induced plant diseases remain a major problem in agriculture, recently exacerbated by global trade and climate change [1, 2]. The most common method of controlling viral infections is the extensive use of chemical pesticides, which target the vectors but often have a nonspecific effect on arthropods and can be harmful to humans [3]. Urgently needed alternative crop protection methods should not only be environmentally sustainable, but also specific, i.e. effective only against a specific target pathogen, and adaptable to the evolution of the pathogen. One strategy to meet these complex requirements is to trigger the RNA silencing component of the plant's immune response against the pathogen [4, 5].

Received: June 4, 2024. **Revised:** January 5, 2025. **Editorial Decision:** February 3, 2025. **Accepted:** March 3, 2025

RNA silencing is a conserved cellular defense mechanism, best characterized in higher eukaryotes, which serves to block (silence) or modulate gene expression at the level of target RNAs. RNA silencing is triggered by double-stranded (ds) regions of RNA molecules. Particularly potent inducers of RNA silencing are nearly completely ds replication intermediates of positive-stranded RNA viruses, the most common class of viral pathogens in plants. Intracellular double-stranded RNA (dsRNA) is perceived by Dicer-like proteins (DCLs), which belong to the type III endonuclease family [6]. Of the four known DCLs in the model plant *Arabidopsis thaliana*, DCL4 and DCL2 have been shown to be of central importance for antiviral RNA silencing [7, 8]. In a process whose molecular details are not yet fully understood, DCL4 and DCL2 hydrolyze dsRNAs into 21 nucleotide (nt) long or 22 nt long small interfering RNAs (siRNAs), i.e. RNA duplexes that are phosphorylated at their 5′ end and have a 2 nt single-stranded overhang with 3′ hydroxyl groups at their 3′ end [6, 9]. The siRNAs become active in RNA-induced silencing complexes (RISCs). The major components of RISCs are Argonaute (AGO) endonucleases, of which AGO1 and AGO2 have been shown to be significantly involved in antiviral RNA silencing [10]. After binding of the siRNA duplex to AGO, one strand, the guide strand, remains bound while the other, the passenger strand, is degraded [11]; AGO1 and AGO2 preferentially incorporate guide strands containing a 5′ terminal U or A nucleotide, respectively [12, 13]. The complementarity of the bound guide strands to the target RNAs is central to the activity of RISC; it is naturally highest for siRNAs that were originally processed by the DCLs from these target RNAs. Association of the RISC with the target RNA then enables AGO-catalyzed endonucleolytic hydrolysis ('slicing') between the nucleotides of the target RNA that are opposite nucleotides 10 and 11 of the siRNA guide strand [14]. RNA silencing directed by siRNAs can thus result in temporary inhibition of gene expression [4]. RISC-mediated slicing of viral RNAs can further enhance the silencing response by inducing the biogenesis of secondary siRNAs via a process that involves host-encoded RNA-dependent RNA polymerases (RDRs) and DCLs [7, 15–17] (Supplementary Fig. S1A).

DsRNAs or siRNAs are already used in crop protection. Several plant varieties have been developed that produce transgenic dsRNA and can thus be protected against viral pathogens or—through targeted RNA silencing of essential messenger RNAs (mRNAs)—against insect vectors and pests, fungi and other pathogens [18–20]. This 'host-induced gene silencing' (HIGS) has the advantage of providing a constant supply of protective dsRNAs throughout the plant's life cycle; however, the production of transgenes is time-consuming and costly, and their release is prohibited in many countries due to safety concerns [18, 21–23]. In addition, transgenic plants can promote the development of resistance and are then potentially susceptible to infection with variants of the pathogen to which they were originally bred for resistance [24]. Alternatively, many encouraging reports suggest that dsRNA suspensions, in the simplest case in the form of a spray [25] (spray-induced gene silencing; SIGS), can be used for topical/transient antipathogenic applications in plants [26]. The prospects for success of these approaches are enhanced by the fact that certain formulations can stabilize the biodegradable RNAs and facilitate their uptake by the plant [23, 27, 28]. Significant progress has also been made in producing dsRNA in gram or kilogram quantities at competitive costs [29]. A first breakthrough recently announced by the US Environmental Protection Agency was the approval of the first dsRNA pesticide Ledprona (CAS number: 2433753-68-3) for 3 years [30].

A major problem with the use of 'RNA actives', as we call antipathogenic siRNA and dsRNAs here, is that both natural and artificially induced RNA silencing processes are generally inefficient. Several independent observations suggest that this is mainly due to the fact that although DCLs generate a large number (a 'pool') of siRNAs from target RNAs, very few of them support AGO-catalyzed RNA cleavage [31–33]. One hypothesis that could explain this is that target RNAs are highly structured and that the association of guide strand/AGO/RISC by complementary base pairing, and thus effective silencing, is only possible in a few regions of the RNA [34, 35], which are referred to here as 'accessible sites', or a-sites [36]. This is particularly relevant when considering the structures of viral genomic RNAs, which have evolved to enable translation and replication, but also to evade RNA silencing by the plant host. Virus-derived siRNAs can even act as decoys by saturating AGO/RISC or silencing cellular targets, facilitating infection [32, 37–40].

To date, artificial dsRNAs consisting of large portions of viral genomes or mRNAs have been used in both transgenic and topical RNA-silencing approaches. It is clear from the above that such dsRNAs have the same application problems as viral RNAs themselves: DCLs generate a large pool of siRNAs, only a few of which are actually active. In other words, many of these dsRNAs turn out to be unusable, and for the dsRNAs that are actually functional, the 'active ingredients' remain unknown. In addition, there is a risk that pool-derived siRNAs may cause 'off-target effects', i.e. the silencing of nontarget RNAs, e.g. by base-pairing of guide strands that are not fully complementary but still sufficient to mediate cleavage [41, 42].

A globally distributed plant virus of major economic importance is *Cucumber mosaic virus* (CMV; family *Bromoviridae*). CMV is transmitted by about 90 aphid species and infects more than 1200 plant species, including a large number of agricultural crops. Symptoms of CMV infections include systemic mosaic symptoms, leaf deformation, systemic necrosis, chlorosis, dwarfism, and fruit damage. Apparently, the virus can persist in the seed over winter and cause primary infections early in the growing season [43–46]. Several CMV-resistant plant species, including tobacco, cucumber, tomato, melon, squash and pepper, have been generated by transgenic approaches [47] using viral dsRNA-expressing constructs, and promising protective effects have also been observed with topical applications of dsRNAs [48–51]. The CMV genome consists of three positive-strand RNA segments (RNA 1, RNA 2, and RNA 3; Supplementary Fig. S1B) that are packaged individually into capsids and cause successful infection when transmitted together. As a result, CMV is capable of reassortment resulting in high mutation rates and antigenic shifts. There is therefore a high risk of loss of resistance in transgenic plants, and particularly high efficacy is essential for topical application of RNA actives.

In previous studies, we and others have established cytoplasmic extracts of cultured *Nicotiana tabacum* BY-2 cells, called BY-2 lysates (BYL), as a versatile experimental tool [52, 53]. BYL supports the *in vitro* translation of (exogenously added) mRNAs into proteins. Most importantly, BYL recapitulates the key steps of primary RNA silencing: i.e. exogenously added dsRNAs are processed by BYL-endogenous

DCLs [33, 54], and functional RISC can be reconstituted with an *in vitro*-translated AGO protein and siRNAs [55, 56]. The activity of the *in vitro*-generated RISC can be tested in a 'slicer assay' that detects AGO-mediated cleavage of a target RNA [55–58] (Supplementary Fig. S1C). Using the BYL system, we have developed a simple *in vitro* experimental method called the '*e*NA screen' to identify nucleic acids, such as siRNA guide strands or DNA antisense oligonucleotides, which can bind to the a-sites of target RNAs and enable efficient endonuclease-catalyzed hydrolysis [33, 36]. From a DCL-generated siRNA pool, *e*NA screening reliably identifies those siRNAs, referred to here as 'effective siRNAs' (*e*siRNAs) that cause efficient AGO/RISC-mediated cleavage of a selected target RNA.

By applying the *e*NA screen to RNAs 2 and 3 of CMV strain Fny, we have identified *e*siRNA*s* that are highly protective against infection by the virus in topical plant protection experiments. Based on these functionally characterized *e*siRNAs, we have developed and designed 'effective dsRNA' (*e*dsRNA) constructs that, when processed by DCLs, produce high levels of these same *e*siRNAs and thus provide significantly better protection against CMV infection than a comparable conventionally organized dsRNA. The tools developed here will help to overcome the lack of efficiency of RNA silencing processes: reliably functional *e*siRNAs and *e*dsRNAs can be generated quickly and flexibly against different RNA targets and used in future RNA-based applications against viral and other plant pathogens.

Materials and methods

Cell culture and preparation of BYL

Nicotiana tabacum BY-2 cells [59] were cultivated at 23°C in Murashige & Skoog liquid medium (Duchefa Biochemie, Haarlem, The Netherlands, #M0221.0025). Protoplasts were generated by treatment with Cellulase RS and Pectolyase Y-23 (Duchefa Biochemie, #C8003 and #P8004) and cytoplasmic extract (BY-2 lysate, BYL) was prepared after evacuolation of protoplasts by percoll gradient centrifugation (Cytiva, Uppsala, Sweden, #17089102) as previously described [52, 53].

Oligonucleotides and siRNAs

DNA oligonucleotides were purchased from Eurofins Genomics (Ebersberg, Germany). The siRNA gf698 targeting GFP mRNA was described earlier [55, 56]. Single-stranded RNA oligonucleotides were synthesized by Biomers (Ulm, Germany). Sequences of DNA and RNA oligonucleotides are listed in Supplementary Table S1. To produce siRNA duplexes, both strands were mixed in siRNA annealing buffer (30 mM HEPES–KOH, pH 7.4, 100 mM KOAc, 2 mM MgOAc) and incubated for 1 min at 90°C and for 60 min at 37°C.

Plasmid construction

To obtain plasmids for the production of *e*dsRNAs or control dsRNAs, a modified pUC18 (Thermo Scientific, Waltham, MA, #SD0051) containing two opposite T7 promoters flanking two BpiI (BbsI) restriction sites was first generated by inserting ds oligonucleotides between the PstI and BamHI sites (Thermo Scientific, #ER0612 and #ER0051) of the vector. Prior to ligation using T4 DNA Ligase (Thermo Scientific, #EL0011), the oligonucleotides were phosphorylated by T4 Polynucleotide Kinase (Thermo Scientific, #EK0031). The plasmids containing the complementary DNAs (cDNAs) of CMV *e*dsRNAs, consisting of several CMV *e*siRNA sequences of 21 or 22 nt length, were then generated by inserting ds oligonucleotides into the BpiI-digested (Thermo Scientific, #ER1011) modified pUC18. The plasmids containing the cDNAs of the control RNAs dsCMV and dsGFP were generated by inserting respective polymerase chain reaction (PCR) products, amplified with Phusion High-Fidelity DNA Polymerase (Thermo Scientific, #F530L) from plasmids pFny209 (see below) or pGFP-C1 (Clontech laboratories, Mountain View, CA), into the BpiI-digested modified pUC18. The resulting plasmids were used to generate PCR products, which served as templates for separate transcription of the two dsRNA strands.

In vitro transcription

Nicotiana benthamiana AGO1L and *AGO2* mRNAs were transcribed *in vitro* from SmiI (SwaI)-linearized (Thermo Scientific, #ER1241) plasmids containing the corresponding open reading frames in a modified pSP64-poly(A) vector (Promega, Madison, WI) with the respective additional restriction site downstream of the poly(A) sequence [56, 57]. Transcription was performed in the presence of monomethylated cap analog m^7GP_3G (Jena Biosciences, Jena, Germany, #NU-852–5) using SP6 RNA Polymerase (Thermo Scientific, #EP0131). Firefly luciferase mRNA was produced by SP6 RNA Polymerase from plasmid pSP-luc(+) (Promega) linearized with XhoI (Thermo Scientific, #ER0692). CMV genomic RNAs (strain Fny) were synthesized with 5′ monomethylated cap analog by T7 RNA Polymerase (Agilent Technologies, Santa Clara, CA, #600 123) from PCR product templates (see Supplementary Table S1 for primer sequences). The template DNAs were amplified with Phusion High-Fidelity DNA Polymerase from plasmids pFny109, pFny209, and pFny309 [60] containing the respective cDNA sequences (kindly provided by Prof. Fernando García-Arenal Rodríguez, Universidad Politécnica de Madrid and Prof. John Carr, University of Cambridge). To generate ds CMV RNA 2, noncapped antisense transcripts were synthesized from PCR products containing the T7 promoter in opposite orientation and subsequently annealed with noncapped sense transcripts. To achieve full complementarity also with the 5′ end of the antisense RNA (starting with guanosine due to the T7 promoter), the 3′ end of the sense RNA used for dsRNA production was changed from the original adenosine to cytidine. The two strands that constitute the *e*dsRNAs or the respective ds control RNAs (dsCMV and dsGFP) were transcribed separately from individual PCR product templates that contained the T7 promoter in opposite orientations. Radioactive labeling of RNAs was performed by *in vitro* transcription in the presence of 0.2 μCi/μl [α-^{32}P]-CTP (3 000 Ci/mmol, Hartmann Analytic, Braunschweig, Germany, #FP-209). Transcripts were treated with RNase-free DNase I (Roche Diagnostics, Mannheim, Germany, #04716728001) and purified by phenol/chloroform extraction and ethanol precipitation or by using the Nucleospin RNA Mini Kit (Macherey-Nagel, Düren, Germany, #740955.50).

Preparation of dsRNA

Annealing of RNAs was performed by mixing equimolar amounts of both single-stranded transcripts in STE ("Salt,

Tris, EDTA") buffer [10 mM Tris–HCl, pH 8.0, 100 mM NaCl, 1 mM ethylenediaminetetraacetic acid (EDTA)], heating for 2 min at 94°C and decreasing the temperature to 25°C within 30 min.

*e*NA screen

Generation and characterization of siRNA pool (see scheme in Fig. 1A). A total of 2.5 µg of the target-dsRNA were incubated for 2 h at 25°C in a 100 µl reaction containing 50% (v/v) BYL, supplemented with 0.75 mM ATP, 0.1 mM GTP, 25 mM creatine phosphate, 80 µM spermine, 0.2 mg/ml creatine kinase (Roche Diagnostics, #10 127 566 001) and 40% (v/v) TR buffer [30 mM HEPES–KOH, pH 7.4, 100 mM KOAc, 1.8 mM MgOAc, 2 mM DTT (Dithiothreitol), cOmplete EDTA-free protease inhibitor cocktail (Roche Diagnostics, #05056489001)]. RNA was isolated from the reaction by treatment with 1 µg/µl Proteinase K (Thermo Scientific, #EO0491) in the presence of 0.5% (w/v) sodium dodecyl sulphate (SDS) for 30 min at 37°C, followed by phenol/chloroform extraction and ethanol precipitation. Purified RNAs from three reactions using different BYL preparations were combined and analyzed by RNA-seq. Data were obtained from three independent experiments.

Characterization of AGO-bound siRNAs (see scheme in Fig. 1C). To generate siRNA-programmed AGO/RISC *in vitro*, 5 pmol *NbAGO1L* mRNA [57] or *NbAGO2* mRNA [61] were translated in the presence of 2.5 µg CMV dsRNA in a 100 µl reaction containing 50% (v/v) BYL under the above-described conditions. Both AGO proteins were produced with an N-terminal FLAG-tag. Samples were mixed with an equal volume of immunoprecipitation buffer [IPB; 20 mM HEPES–KOH, pH 7.6, 150 mM NaCl, 0.5% (v/v) NP-40, 1 mM DTT] containing 20 µl Anti-FLAG M2 affinity gel (Sigma-Aldrich, St. Louis, MO, #A2220). Following overnight incubation at 4°C with gentle agitation, the resin was washed three times with IPB, once with IPB containing 300 mM NaCl and a final time with IPB. RNA was isolated using proteinase K treatment, phenol/chloroform extraction and ethanol precipitation. Purified RNAs from three reactions using different BYL preparations were combined and analyzed by RNA-seq. Data were obtained from three different experiments, except for the AGO 1 IP with CMV RNA 2-derived siRNAs (two experiments).

***In vitro* slicer (cleavage) assay** (see scheme in Supplementary Fig. S1C). AGO/RISC programmed with a specific siRNA were generated as described above in a 20 µl reaction containing 50% (v/v) BYL, 0.5 pmol *NbAGO1L* or *NbAGO2* mRNA, 100 nM CMV siRNA duplex or 200 ng *e*dsRNA. After 2.5 h at 25°C, 2 µg of firefly luciferase mRNA (serving as competitor RNA for nonspecific acting RNases in BYL) and the ^{32}P-labeled target RNA (10 fmol) were added, and the cleavage reaction performed for 15 min. Total RNA was isolated by treating the reaction with 20 µg Proteinase K in the presence of 0.5% SDS for 30 min at 37°C, followed by chloroform extraction and ethanol precipitation. RNAs were separated on 1.5% denaturing agarose gels, ^{32}P-labeled target RNAs and cleavage products were visualized by phosphor-imaging. To determine cleavage efficiencies of *e*siRNA candidates, the band intensities of the original, uncleaved transcripts were quantified with ImageQuant TL (Cytiva), data were obtained from two different experiments.

RNA-seq and bioinformatic analysis

RNA-seq was performed with an Illumina NextSeq 550 (BYL samples) or Illumina NovaSeq 6000 (*N. benthamiana* samples) in the Core Unit DNA Technologies at the University of Leipzig (Germany), using the NEXTFLEX® Small RNA-Seq Kit v3 (Bioo Scientific, Austin, TX, #5132-05) or v4 (Revvity, Waltham, MA, #NOVA-5132-32) to prepare the small RNA libraries. Adapter sequences were clipped from the raw reads using cutadapt 3.2 [62] with parameters specifying a maximum allowed error rate of 0.2 when matching adapters, a minimum overlap of 5 nt between adapter sequence and read, and a quality cutoff of 20 on the Phred-score from either end of the read, filtering for a minimum length of 15 nt of the adapter clipped reads (-e 0.2 -O 5 -q 20,20 -m 15). Since sequenced fragments were ligated with 4 nt random sequences at both ends prior to library preparation for the BYL samples, additional four bases were cut from both ends of the adapter-clipped reads using cutadapt, again filtering for a minimum read length of 15 nt. Reads were mapped to the respective CVM RNAs using bowtie 1.3.0 [63]. To this end, a bowtie index was generated including the chromosome and scaffold sequences of the *N. tabacum* Nitab 4.5 genome sequence [64] available from https://solgenomics.net/ftp/genomes/Nicotiana_tabacum/edwards_et_al_2017/assembly/ or the *N. benthamiana* 2.6.1 genome [65] available from https://solgenomics.net/ftp/genomes/Nicotiana_benthamianaV261/Nbenthamiana_Assembly/, respectively, to avoid false-positive mappings of fragments originating from the cytoplasmic extract to the CMV RNAs. The bowtie command line was specified with additional parameters (–best –all –strata –tryhard -n 3) to achieve high mapping sensitivity. Reads mapping to the respective CMV RNA were extracted using samtools view 1.11 [66] for further processing, while reads mapping to the Nitab 4.5 or Niben 2.6.1 sequences were discarded. Using custom Java and R scripts applied to the mapping result for each library, 5′ ends of reads mapping to the respective CMV RNA were counted position-wise, separately for each mapping strand and separately for each length fraction between 19 and 26 nt. Resulting count values were further used for determining the length distribution of mapped reads, the preference for 5′ nucleotides (based on the CMV RNA sequence), position-specific read counts and siRNA-specific read counts. Log_2 fold changes between AGO1/AGO2 IP samples and DCL-processed siRNA pools were determined based on average count values, normalized to total library size per length fraction and treatment. Due to substantially different library sizes of replicates, normalization was performed prior to averaging in case of CVM RNA 3.

RNA inoculation/CMV challenge of plants

Mechanical co-inoculation of siRNAs or dsRNAs and CMV genomic RNAs was performed with 4–5 week-old *N. benthamiana* plants obtained from the Leibniz Institute of Plant Biochemistry in Halle (Saale), Germany. Plants were grown in a chamber (CLF Plant Climatics, Wertingen, Germany) under daily conditions of 14 h at 23°C, 90–100 µmol m^{-2} s^{-1} light (at shelf level) and 10 h at 21°C in the dark.

Prior to the application of the RNAs, the upper surface of the third and fourth leaf was dusted with carborundum powder (silicon carbide, Sigma–Aldrich, #37809-7). To analyze the processing of *e*dsRNAs *in planta*, 5 µl solution

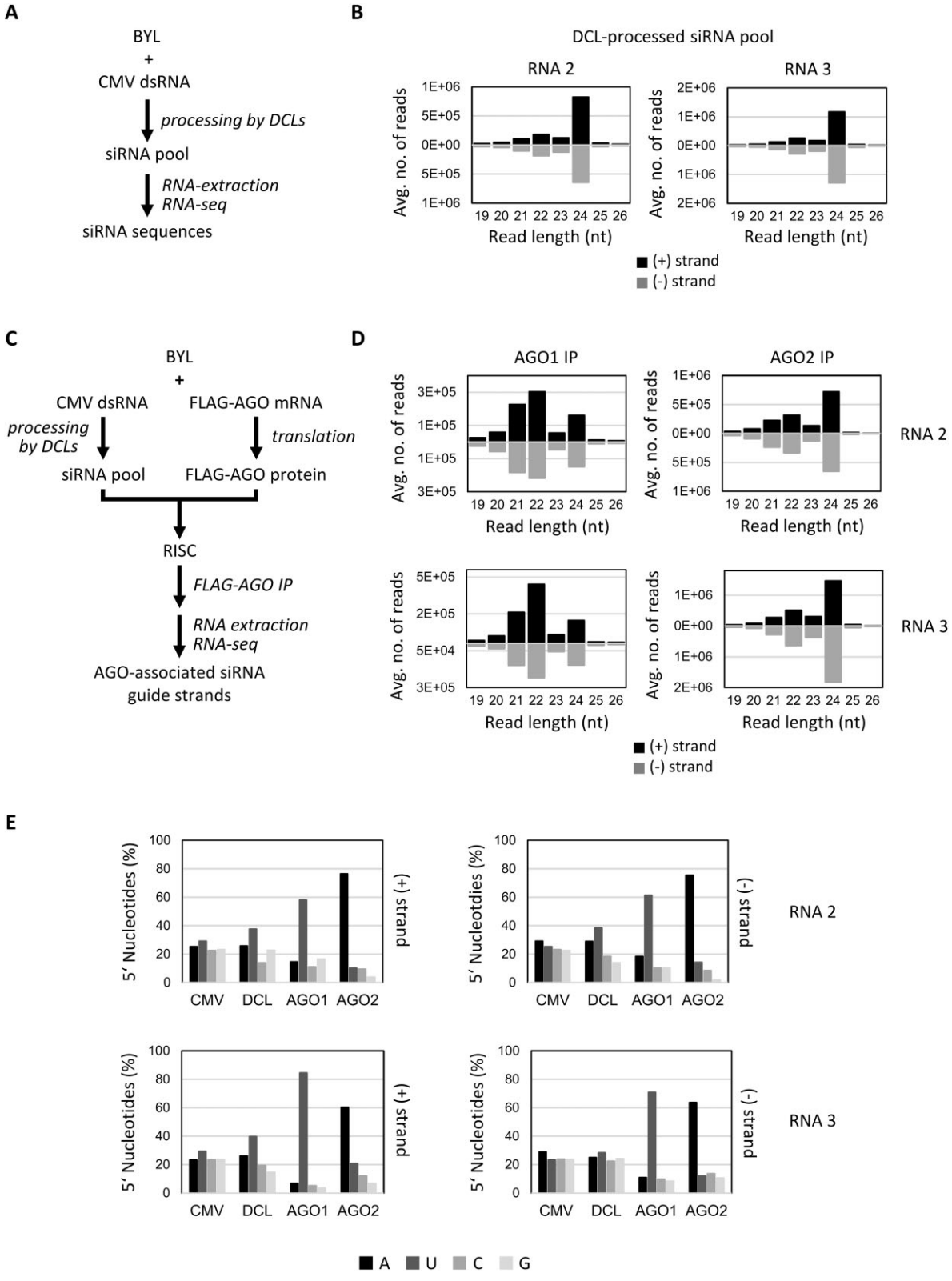

Figure 1. Identification and characterization of *e*siRNA candidates from CMV Fny RNAs 2 and 3 (*e*NA screens, steps 1 and 2). (**A**) Schematic of the siRNA pool generation and characterization procedure (see text for details). (**B**) Size distribution of siRNAs generated by the BYL-endogenous DCLs from dsRNA versions of CMV RNAs 2 and 3. Bars above and below the axis represent siRNAs derived from viral (+) and (−) strand RNA, respectively. Data represent the mean of three experiments. (**C**) Schematic representation of the procedure to identify AGO-bound siRNAs (see text for details). (**D**) Size distribution of CMV siRNAs isolated from AGO immunoprecipitations (IP). Data represent the mean of three experiments, except for AGO1 IP with CMV RNA 2 siRNAs (two experiments). (**E**) Relative abundance of the respective 5′ terminal nucleotides of the AGO1- and AGO2-associated 21 nt siRNA guide strands. The abundance was compared with the nucleotide compositions of the respective CMV RNAs (CMV), and the relative abundance of the 5′ terminal nucleotides of all sequenced 21 nt CMV siRNAs generated in BYL by endogenous DCLs [DCL; see panels (A) and (B)]. Identified *e*siRNA candidates from CMV RNA 2 and CMV RNA 3 are listed in Tables 1 and 2, respectively.

containing 70 pmol (ca. 8 μg) of dsCMV6-21 or dsCMV6-21o were mixed with an equal volume of inoculation buffer (30 mM K_2HPO_4, pH 9.2, 50 mM glycine) and 2.5 μl were rubbed onto each leaf half using a pipette tip and, after 10 min, the inoculated leaves were rinsed with water. Leaf material was collected from treated areas 4 h after dsRNA inoculation, and total RNA was isolated using TRIzol reagent (Thermo Scientific, #15596026) according to the manufacturer's instructions. Small RNAs were analyzed by RNA-seq as described before.

For CMV challenge experiments, 5 μl solution containing *in vitro* transcribed CMV RNAs 1, 2, and 3 (20 fmol each) and siRNA (150 pmol, if not indicated differently) or dsRNA (70 pmol, if not indicated otherwise) were mixed with an equal volume of inoculation buffer and applied to the plants as described above. The plants were monitored daily for up to 70 days for the development of symptoms (see information on time frames in the individual figures). Finally, leaf material was collected from representative symptomatic and asymptomatic plants and total RNA was isolated as described above. Data were obtained from at least two different experiments (see figures for number of plants), except for the control experiment with the single-stranded RNAs constituting the CMV *e*dsRNA (Supplementary Fig. S7B).

Results

Identification of *e*siRNAs targeting CMV RNAs 2 and 3

CMV RNAs 2 and 3 were selected as targets for our antiviral approach because these genome segments each encode two proteins essential for the infectious viral life cycle. CMV RNA 2 encodes the viral RDR 2a and, via the subgenomic RNA 4A, the viral suppressor of RNA silencing (VSR) 2b. CMV RNA 3 encodes the movement protein (MP) 3a and, via the subgenomic RNA 4, the viral capsid protein CP (Supplementary Fig. S1B).

To obtain *e*siRNAs, we adapted a previously developed protocol for the *e*NA screen [33] (see the 'Materials and methods' section for details), which consists of three steps that are summarized here and explained in detail in the following sections. (i) Delivered as dsRNA, the target RNA of choice was exposed to BYL for processing by endogenous DCLs to produce a pool of siRNAs. Next-generation sequencing (RNA-seq) monitored the entire siRNA population (scheme in Fig. 1A). (ii) In BYL containing such a siRNA pool, RISCs were reconstituted with an AGO protein of choice. AGO was translated *in vitro* from a cognate (*in vitro* transcribed) mRNA. Formed AGO/RISC were immunoprecipitated, and the bound siRNA strands were identified by RNA-seq (scheme in Fig. 1C). The RNA-seq data obtained in step (i) were then used for comparison to define enrichment in the AGO/RISC. (iii) From the siRNAs detected in step (ii), those siRNAs that induced efficient slicing of the target RNA were finally identified by BYL-supported slicer assays that test for endonucleolytic cleavage of the target RNA (see Supplementary Fig. S1C for assay scheme).

Applying this approach to CMV, full-length sense and antisense transcripts were generated from cDNA clones of RNAs 2 and 3 of the Fny strain [60] and hybridized (see the 'Materials and methods' section). The resulting dsRNAs were processed from BYL-endogenous DCLs, and the generation of small RNAs was determined qualitatively by gel electrophoresis and quantitatively by RNA-seq (Supplementary Fig. S2A and B and Fig. 1B). In close agreement with previous *e*NA screens [33], siRNAs with lengths of 21–24 nt were detected, with the ratio of siRNAs generated from the positive- and negative-orientated strands of the dsRNAs being balanced. Consistent with previous observations, siRNAs of 24 nt were found to be the predominant type (Fig. 1B) suggesting that DCL3, which processes dsRNA into 24 nt long siRNAs, is more abundant or more active in BYL than DCL2 and DCL4. Since 21 nt siRNAs were of particular interest due to their documented antiviral activity, we analyzed the average frequency with which a 21 nt siRNA was processed at a specific position of the respective dsRNA versions of genomic CMV RNAs 2 and 3. The data showed that DCL processing occurred along the entire length of the RNAs, with slightly higher frequencies at certain sites (Supplementary Fig. S2B). Analogous to data previously obtained with dsRNA of the genome of Tomato bushy stunt virus (TBSV), which is not related to CMV, this behavior of DCL4, the enzyme most likely involved here, could not be explained by any general rule, except for a certain preference for cleavage at the RNA termini and at GC-rich sequence motifs [33, 67] (data not shown).

To identify those virus-derived siRNAs whose guide strands are preferentially bound by the AGO1 and AGO2 proteins, we repeated the generation of the CMV RNA-derived siRNA pools and then exposed the siRNAs to AGO1 (AGO1L variant from *N. benthamiana*) [57] or AGO2 (from *N. benthamiana*) [61], which were translated *in vitro* in BYL. The AGOs were produced with an N-terminal FLAG tag, which allowed IP of the proteins including the bound siRNAs. Successful translation and IP of the FLAG-AGO proteins was verified as well as co-precipitation of DCL-processed siRNAs with the corresponding FLAG-AGO (Supplementary Fig. S2C and D). Subsequent RNA-seq of the precipitated siRNAs revealed a massive enrichment of 21 and 22 nt siRNAs compared to 24 nt siRNAs, especially with AGO1, but also AGO2 (compare Fig. 1D and B). Consistent with the known preferences of AGO proteins for binding siRNA guide strands, the vast majority of siRNAs bound by AGO1 had a 5′ terminal uridine, whereas siRNAs bound by AGO2 predominantly had a 5′ terminal adenosine (Fig. 1E and Supplementary Table S2). Further analyses of the RNA-seq data focused on 21 nt siRNAs that were significantly enriched in the respective AGO/RISC and whose guide strands had negative strand polarity, i.e. they were complementary to the CMV genomic RNAs. Thus, siRNAs were selected that were highly enriched in the precipitated AGO/RISC compared to the DCL-processed siRNA pool, or siRNAs that were only detected in the IP samples but not in the original siRNA pool: both criteria indicated a high affinity of the siRNA to the corresponding AGO protein. In the case of CMV RNA 2, these were 12 AGO1- and 14 AGO2-bound siRNAs; in the case of CMV RNA 3, these were 11 AGO1- and 13 AGO2-bound siRNAs, which were considered for further study (Supplementary Table S2 and Tables 1 and 2). For unknown reasons, some of the candidates contained a 5′ terminal nucleotide that did not match AGO1's and AGO2's major preferences (Supplementary Table S2). Tests with examples of these siRNAs (e.g. siR1844) showed that they were not functional (Fig. 2, and data not shown). Therefore, from the outset, siRNAs were excluded from further analysis if their 5′ nucleotides did not match the AGO-specific preferences. Nevertheless, the observation that viral siRNAs with a nonpre-

Table 1. *e*siRNA candidates targeting CMV RNA 2

siRNA[a]	Guide strand (5′–3′)	Passenger strand (5′–3′)	*In vitro* cleavage efficiency (%)[b]	Symptom-free plants (%)[c]
		Screening via AGO1		
149	UCGACACCGUAACUGCCGUUC	ACGGCAGUUACGGUGUCGACA	63[d]	ND
186	UUGCUCAGAUCGCAAACGUUC	ACGUUUGCGAUCUGAGCAACG	37[d]	ND
359	UCAGAUUUUUCAAGGUAAUCU	AUUACCUUGAAAAAUCUGAUG	90	93
1172	UUACGUUUCUUAAUUGCUGUA	CAGCAAUUAAGAAACGUAAUG	96	100
1489	UACUCUUCUUAUGAUACGUUA	ACGUAUCAUAAGAAGAGUAUA	96	93
1613	UUGACAUCAAAUCCUGCCAUC	UGGCAGGAUUUGAUGUCAAGA	94	ND
1844	GUAUUGCCAAAAUAAGUGAGU	UCACUUAUUUUGGCAAUACCA	7	0
1982	UUGAAAAGAGUUGUGAAUUUA	AAUUCACAACUCUUUUCAACA	84	ND
2441	UUGCACCUACGUUCAAUUCCA	GAAUUGAACGUAGGUGCAAUG	75	ND
2562	UUUGAACGCGCUCUCUCGCUG	GCGAGAGAGCGCGUUCAAAUC	72	ND
2727	UUACCGGCGAACCAAUCUGUA	CAGAUUGGUUCGCCGGUAACG	72	ND
2740	UUCCGCCCAUUCGUUACCGGC	CGGUAACGAAUGGGCGGAAGG	13	ND
		Screening via AGO2		
380	AAAGCGACAAGGAGCUCAUCA	AUGAGCUCCUUGUCGCUUUUG	89	60
407	AUACGCAUGGGUUUGACCAUC	UGGUCAAACCCAUGCGUAUCG	82	ND
449	AUAAAAGAACAUUUAUUAAAC	UUAAUAAAUGUUCUUUUAUUU	82	ND
540	AAUAGCCGCGACCAGGUCUUC	AGACCUGGUCGCGGCUAUUUA	60	ND
557	AAAUCAGAUUUAGUGUAAAUA	UUUACACUAAAUCUGAUUUCU	64	ND
1020	AUAGUCUGCACUUUCGACGAA	CGUCGAAAGUGCAGACUAUUC	93	100
1054	ACUGUCGAAGUCUAACAUGAU	CAUGUUAGACUUCGACAGUCU	89	ND
1248	AAUGAAGAAUCUCUCAGCCAC	GGCUGAGAGAUUCUUCAUUUC	90	ND
2041	AGAGUAAGAACUUCGAACAAA	UGUUCGAAGUUCUUACUCUCU	87	60
2634	ACAUGGCGGCAUGACCCUGUC	CAGGGUCAUGCCGCCAUGUGA	0	7
2748	AAAGCACCUUCCGCCCAUUCG	AAUGGGCGGAAGGUGCUUUCU	0	ND
2801	ACUCAGCUCCCGCCACAGAAA	UCUGUGGCGGGAGCUGAGUUG	0	ND
2863	AUGGACAACCCGUUCACCACA	UGGUGAACGGGUUGUCCAUCC	0[d]	ND
2955	AAACCUAGGAGAUGGUUUCAA	GAAACCAUCUCCUAGGUUUCU	0[d]	ND

[a]siRNAs in italics are not considered *e*siRNA candidates.
[b]Percentage of target RNA cleaved in standard slicer assays in BYL. Values represent the average of two independent experiments.
[c]ND: not determined.
[d]Efficiency of cleavage may be underestimated due to a similar size of uncleaved target and one of the cleavage products.

ferred 5′ end can also efficiently bind to AGO1 and AGO2 was interesting: we hypothesize that at least some of these siRNAs may have a decoy function.

When tested *in vitro* for slicer/target cleavage activity, most, but not all, of the selected siRNAs mediated substantial cleavage of the CMV RNAs 2 and 3 (Fig. 2). In fact, based on data from various *in vitro* screening studies, the majority of these siRNAs met the arbitrary definition of an '*e*siRNA candidate': accordingly, a candidate *e*siRNA was defined here as one that induces hydrolysis of more than 25% of a target RNA in a standardized *in vitro* slicer assay with appropriate AGO/RISC compared to a control reaction without siRNA (Fig. 2; also see the 'Materials and methods' section). For example, based on their cleavage activity, siR359, siR1172, and siR1489 were identified as *e*siRNA candidates with AGO1 on CMV RNA 2 (candidates are named with 'siR' and the position of the viral positive-strand RNA to which the 5′-nucleotide of the siRNA guide strand is complementary). Similarly, siR380, siR1020, and siR2041 were identified as highly cleavage-active siRNA candidates with AGO2/RISC (Table 1). Examples of *e*siRNA candidates that acted with AGO1 on CMV RNA 3 were siR239, siR507, and siR985; with AGO2 they were siR593, siR1019, and siR1569 (Table 2). In general, however, both the total number and the cleavage efficiencies of the *e*siRNA candidates identified for CMV RNA 3 were significantly lower than for CMV RNA 2 (Fig. 2 and Tables 1 and 2).

Identified *e*siRNAs show high antiviral activity *in planta*

Subsequently, the antiviral (protective) activity of some of the identified *e*siRNA candidates was tested *in vivo*. For this purpose, *N. benthamiana* plants (n = 12–15) were treated with carborundum using a standard protocol ('rub-inoculation') and 150 pmol (~1 µg) of the (synthesized) siRNA to be tested. At the same time, 20 fmol of each of the CMV genomic RNAs 1–3, prepared by *in vitro* transcription from full-length cDNAs, were inoculated per plant. It is important to note that this amount of CMV Fny RNAs, when inoculated into *N. benthamiana* plants without the addition of antiviral siRNAs was previously confirmed to result in infection of 100% of the plants with significant symptom development and pathogenesis, including deformed leaves and severe dwarfism. This means that the plants were subjected to what we refer to as a 'maximally successful challenge' by the virus. First, the 21 nt long siRs 359, 380, 1020, 1172, 1489, and 2041 derived from CMV RNA 2 were used. As a negative control, we applied siR gf698, a nonspecific siRNA-targeting green fluorescent protein (GFP) mRNA. In addition, we used two siRNAs, siR1844 and 2634, which showed no, or low, cleavage activity on the target RNA in the previous slicer assays (Fig. 2 and Table 1). Fig. 3A shows representative images of plants treated as described above and examined for symptom development at a maximum of 35 days post-inoculation (dpi); Fig. 3B shows the overall progression over several independent

Table 2. *e*siRNA candidates targeting CMV RNA 3

siRNA[a]	Guide strand (5′–3′)	Passenger strand (5′–3′)	*In vitro* cleavage efficiency (%)[b]	Symptom-free plants (%)[c]
		Screening via AGO1		
151	UUAAAGUCCUACUGGUACCUU	GGUACCAGUAGGACUUUAACU	31[d]	ND
239	UCACACUCAGUAGCCAUUUUC	AAAUGGCUACUGAGUGUGACC	75[d]	33
507	UAACGAAACGCAUUGCCCAUC	UGGGCAAUGCGUUUCGUUACA	70	33
985	UUAUAUACUAAUACGCACCAA	GGUGCGUAUUAGUAUAUAAGU	87	20
988	UACUUAUAUACUAAUACGCAC	GCGUAUUAGUAUAUAAGUAUU	79	ND
1098	UUACUAAAACCAGAUGUGUUC	ACACAUCUGGUUUUAGUAAGC	41	ND
2061	UUCUCCACGACUGACCAUUUU	AAUGGUCAGUCGUGGAGAAAU	16	17
2174	UACCCUGAAACUAGCACGUUG	ACGUGCUAGUUUCAGGGUACG	16	ND
		Screening via AGO2		
35	ACACACACACGCACACACACA	UGUGUGUGCGUGUGUGUGUGU	44[d]	ND
358	AUUCACCAACAUCAUAUCCAG	GGAUAUGAUGUUGGUGAAUUA	67	ND
478	AUAACUCCUUGUCGCCCAGAU	CUGGGCGACAAGGAGUUAUCU	63	ND
496	AUUGCCCAUCUAUGGGAGAUA	UCUCCCAUAGAUGGGCAAUGC	77	ND
592	AACACCGCUUACGAUUCCCAA	GGGAAUCGUAAGCGGUGUUUU	86	ND
593	AAACACCGCUUACGAUUCCCA	GGAAUCGUAAGCGGUGUUUUG	90	33
733	AAGGCAGUACUAGAGUCUUCC	AAGACUCUAGUACUGCCUUUC	78	ND
1019	AUAGAUAUAGUAUUAUGUACA	UACAUAAUACUAUAUCUAUAG	88	53
1132	AAGAGGAAUUGAACCUCAAAA	UUGAGGUUCAAUUCCUCUUAC	20	0
1394	AACGUCUUAUUAAGUCGCGAA	CGCGACUUAAUAAGACGUUAG	24	ND
1569	AACAAGCUUCUUAUCAUAUUC	AUAUGAUAAGAAGCUUGUUUC	74	7
2099	AAGGCGCCUCAGAGAUUUGUA	CAAAUCUCUGAGGCGCCUUUG	15[d]	ND

[a]siRNAs in italics are not considered *e*siRNA candidates.
[b]Percentage of target RNA cleaved in standard slicer assays in BYL. Values represent the average of two independent experiments.
[c]ND: not determined.
[d]Efficiency may be underestimated due to a similar size of uncleaved target and one of the cleavage products.

infection/protection experiments (three independent experiments including 3–5 plants per treatment/per experiment). It was found that siR359 and siR1489 each provided 93% protection and siR1020 and siR1172 each provided 100% protection against CMV infection, indicating that all, or the vast majority, of the plants treated in this way remained symptom-free. siR380 and siR2041 provided 60% protection against CMV infection, meaning that 40% of these plants developed symptoms. The control siRNA and, importantly, the two siRNAs that were inactive in previous slicer assays provided little or no protection; since none, or very few (7%), of the plants treated in this way remained symptom-free (Fig. 3A and B). These results show that the observed protective effect of siRs 359, 380, 1020, 1172, 1489, and 2041 was indeed due to RNA silencing processes in the plant. In other words, we concluded that the protective effect was not triggered by single-stranded siRNA guide strands that might still be present as contamination in the siRNA preparations and could hybridize to the corresponding viral RNA strands during the inoculation process (see also below). Protection was also confirmed by the fact that genomic CMV RNA was no longer detectable by reverse transcriptase-polymerase chain reaction in plants identified as asymptomatic at 35 dpi (Supplementary Fig. S3; all data summarized in Table 1).

The equivalent experiment with the candidates characterized from CMV RNA 3 showed that protection against CMV infection could also be achieved here. However, the level of protection was clearly lower than with the *e*siRNA candidates from CMV RNA 2 (Fig. 3C and D; summarized in Table 2). This was expected, as most of these siRNAs directed against CMV RNA 3 showed a lower slicer activity *in vitro* (Fig. 2 and Tables 1 and 2). Note that an *e*siRNA directed against CMV RNA 2, siR359, was also tested in the experiments shown in Fig. 3C and D, and it provided comparable protection to the infection experiments shown in Fig. 3A and B. This demonstrates the high degree of reproducibility of these experiments.

Like 21 nt siRNAs, 22 nt siRNAs were previously shown to play an important role in establishing effective RNAi responses [15, 68]. Accordingly, we next wanted to know whether a comparable antiviral protection could be achieved with 22 nt versions of the previously characterized *e*siRNAs (guide strands extended by 1 nt). In slicer assays, the 22 nt siR359, siR1172, siR1489, siR380, siR1020, and siR2041 were found to have similar or slightly lower activity in the respective AGO/RISC on the target RNA (Supplementary Fig. S4A). Plant protection experiments with the 22 nt siR359 and siR1020 showed a similar tendency: i.e. the protection levels were either similar (siR359) or reduced (siR1020) compared to those of the 21 nt *e*siRNAs (exemplarily shown in Supplementary Fig. S4B and C).

Thus, from an undefined siRNA pool, *e*NA screening reliably characterized *e*siRNAs that were functional, i.e. highly effective in topical antiviral applications; 21 nt versions were more potent than 22 nt versions of these *e*siRNAs, and CMV RNA 2-derived *e*siRNAs were more potent than CMV RNA 3-derived *e*siRNAs.

‘Multivalent’ dsRNAs, ‘*e*dsRNAs’, composed of the sequences of several *e*siRNAs, are highly effective in protecting plants against CMV infection

For crop protection applications, dsRNAs are considered a better choice than siRNAs, because they are significantly cheaper to produce [23] and more stable [69]. As mentioned

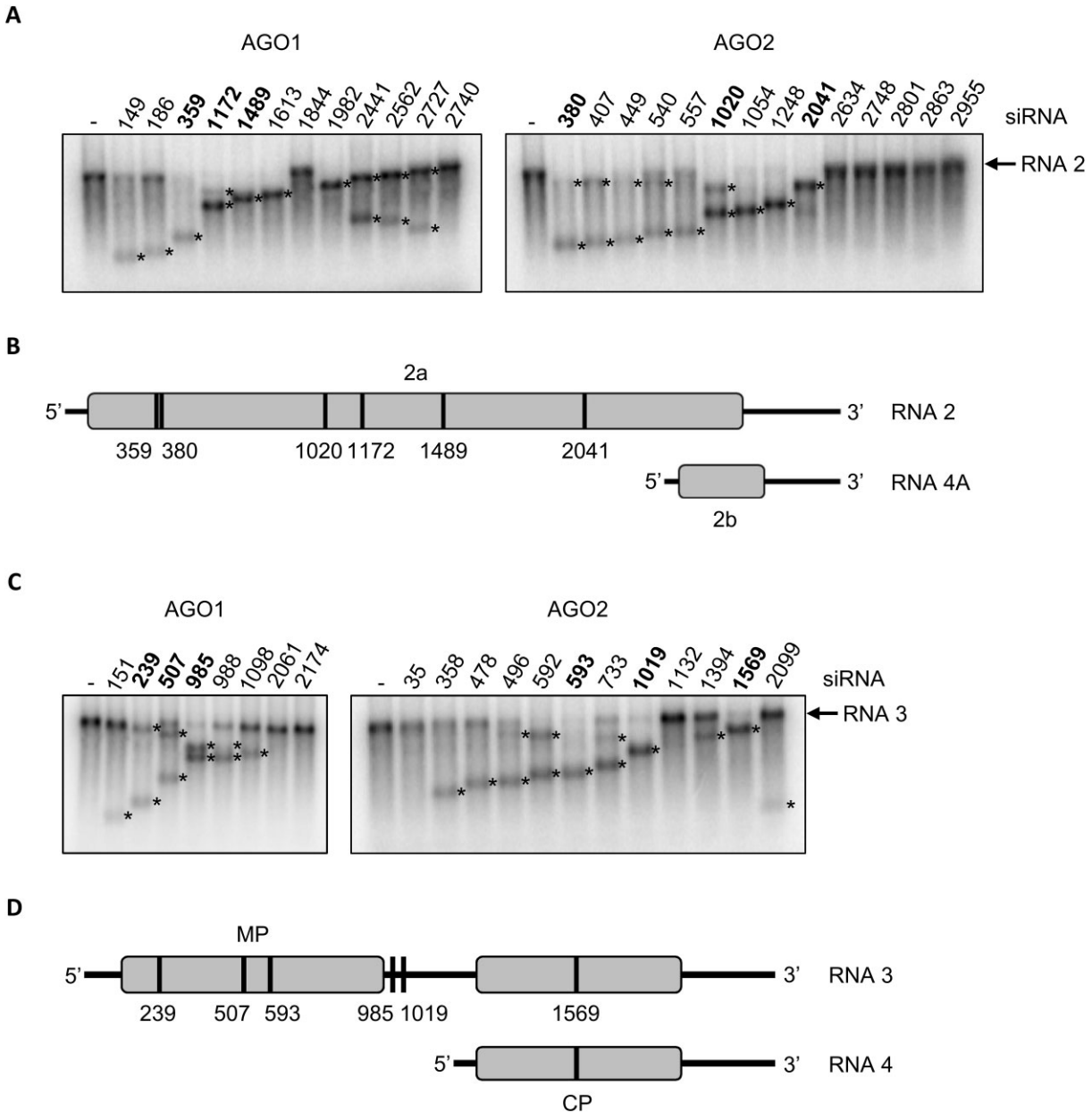

Figure 2. RNA silencing activity of *e*siRNA candidates *in vitro* (*e*NA screens step 3). Slicer assays with the *e*siRNA candidates identified in step 2 of the *e*NA screen and CMV RNAs 2 or 3 (Fig. 1) were performed as shown schematically in Supplementary Fig. S1C and described in the text. The numbers of the *e*siRNA candidates correspond to the designations given in the text, tables, and figures below. Asterisks (*) denote the cleavage products. The fact that in some cases only one cleavage product was detected can be explained by co-migration of larger cleavage products with the target RNA, weak labeling of smaller cleavage products and/or by different stabilities (especially of the 3′ cleavage products) with respect to further degradation by RNases. Determined slicing efficiencies are summarized in Tables 1 and 2. (**A**) Representative slicer assays performed with *e*siRNA candidates, CMV RNA 2 and AGO1/RISC or AGO2/RISC. Six *e*siRNA candidates (three active with AGO1, three active with AGO2) that were further investigated are shown in bold. (**B**) Schematic representation of the binding sites of these siRNAs on CMV RNA 2. (**C**) Representative slicer assays performed with *e*siRNA candidates, CMV RNA 3 and AGO1/RISC or AGO2/RISC. *e*siRNA candidates that were further investigated are shown in bold. (**D**) Binding sites of these siRNAs on CMV RNA 3.

above, currently used antiviral dsRNAs consist only of complementary long, contiguous regions of viral genomic RNA. From these, few, if any, *e*siRNAs were produced during the DCL-mediated processing. In addition, many other nonfunctional or undesirable (e.g. potentially 'off-targeting') siRNAs were produced (see also the 'Discussion' section). After the successful identification of *e*siRNAs against CMV, the use of dsRNAs containing several *e*siRNA sequences seemed particularly promising; DCLs should generate the constituent *e*siRNAs, and the corresponding RISCs should then attack the target RNA at different a-sites to hydrolyze it with maximum efficiency. Therefore, engineering cDNAs to produce '*e*dsRNAs' that are effective against CMV was the next step in this study.

It was particularly important to ensure that the *e*siRNAs that compose the *e*dsRNA are actually produced by the DCLs, especially since the way in which plant DCLs enzymatically convert dsRNA substrates is incompletely characterized

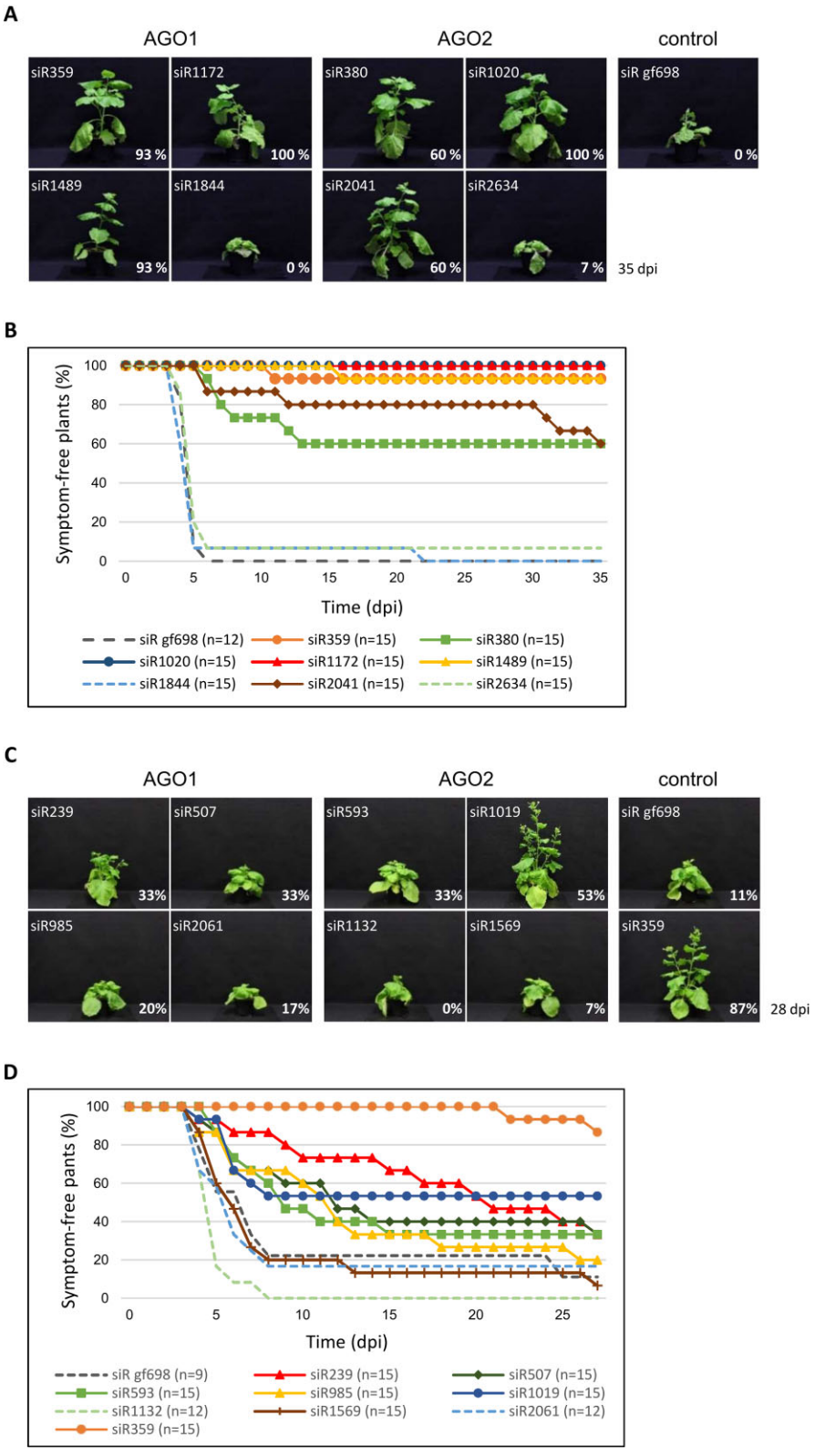

Figure 3. Identified *e*siRNAs protect plants efficiently against CMV infection. *Nicotiana benthamiana* plants were mechanically co-inoculated with the individual synthetic *e*siRNA candidates and with the genomic CMV RNAs 1, 2, and 3. The concentration of the viral RNAs was chosen to achieve a maximal successful challenge with the pathogen (see text). siRNA gf698 targeting GFP mRNA was used as a negative control. Plants were monitored for the appearance of CMV-specific symptoms for at least 28 dpi. (**A, C**) Representative plant images illustrate the differences between asymptomatic and symptomatic individuals at 35 dpi (RNA 2-targeting siRNAs) or at 28 dpi (RNA 3-targeting siRNAs). The percentage of plants remaining asymptomatic is given for each siRNA. (**B**) Percentage of asymptomatic plants over the entire course of the experiment with RNA 2-targeting siRNAs. Results are from three independent experiments with 4–5 plants each, the total number of plants is indicated ($n = 12$–15). (**D**) Percentage of asymptomatic plants over the entire course of the experiment with RNA 3-targeting siRNAs. Results are from three independent experiments with 3–5 plants each, the total number of plants is indicated ($n = 9$–15). An *e*siRNA directed against CMV RNA 2 (siR359) was used as an additional control.

(see Introduction section). Previous and recent observations [70–72] support the hypothesis that DCLs should be active at both ends of a dsRNA and endonucleolytically hydrolyze the RNA from there, possibly in a phased pattern. Based on these considerations, cDNAs were constructed from which complementary RNA strands were transcribed that formed *e*dsRNAs by annealing. These cDNAs contained the sequences of six of the previously characterized 21 or 22 nt *e*siRNAs 1172, 1489, 359 and 1020, 2041, 380, respectively, with the sequences of the guide strands of three *e*siRNAs arranged in opposite directions initiating from the respective 5′ end (see Fig. 4A and Supplementary Fig. S5). To obtain intact double strands, the 2 nt overhangs of the passenger strands of *e*siRNAs 359, 380, and 2041 were modified to match the corresponding complementary bases.

As an additional feature of *e*dsRNA-encoding cDNAs, we have introduced 21 or 22 nt long, so-called 'pseudo-siRNA sequences' (Fig. 4A). These served two purposes: at the cDNA level, these elements contained consensus sequences (+1 to + 6) that promote T7 RNA polymerase-mediated transcription; otherwise, the nucleotide composition was random. Both *e*dsRNA strands could be generated accordingly by *in vitro* transcription. At the RNA level, we hypothesized that the presence of the appropriate length pseudo-siRNA sequences should support the proper processing of the downstream *e*siRNA components. Assuming that DCL4, like other DCLs and Dicers, acts in a processive manner using the 5′-counting rule [6, 70, 73], the 21 nt long *e*siRNAs should preferentially result from DCL4 activity on this substrate if the pseudo-siRNAs are 21 nt long. A similar scenario was expected for DCL2 and edsRNA substrates with terminal 22 nt pseudo-siRNA sequences. The cDNAs encoding the 21 or 22 nt pseudo-siRNAs and *e*siRNAs were used to generate PCR products that served as templates for separate *in vitro* transcription of the single-stranded components of the dsRNA. Subsequently, the transcripts were hybridized to obtain the dsRNA. By using different PCR primers, we generated dsRNAs with blunt ends (here referred to as dsCMV6-21 or dsCMV6-22; see also Fig. 4A and Supplementary Fig. S5 for the sequence composition), or dsRNAs with 2 nt long 3′ overhangs (here referred to as dsCMV6-21o or dsCMV6-22o). The latter variants were developed based on reports suggesting that DCLs on dsRNAs with overhangs show more precise processing [70, 74].

First, we tested the DCL-mediated processing of the constructed *e*dsRNAs. To do this, we again used the endogenous DCL activities in BYL; in analogy to the experimental procedure shown in Fig. 1A, labeled *e*dsRNAs were added to BYL and the processing to siRNAs was monitored over a period of 24 h. For example, with dsCMV6-21o, we obtained a processing pattern indicating the generation of 21 nt siRNAs. However, in line with the fact that BYL contains not only active DCL4 but also DCL3, significant amounts of 24 nt-long siRNAs were also generated (Fig. 4B).

Next, we tested the *e*dsRNAs in a slicer assay. Analogous to the previous procedure (Fig. 4B), the *e*dsRNAs were processed in BYL by the endogenous DCLs. AGO1/RISC or AGO2/RISC were reconstituted with the resulting siRNAs and slicing of CMV RNA 2 target was analyzed (Supplementary Fig. S1C). The assays with the *e*dsRNAs were performed side-by-side with the individual *e*siRNAs or with a mixture of the respective *e*siRNAs. As shown in Fig. 4C with dsCMV6-21o, efficient hydrolysis of CMV RNA 2 occurred in all cases, i.e. the target RNA was almost completely degraded to the corresponding cleavage products. Furthermore, efficient cleavage was obtained regardless of whether the *e*dsRNAs were composed of 21 or 22 nt *e*siRNA sequences and whether they contained a 2 nt overhang or not (Supplementary Fig. S6). Systematic testing revealed that ∼0.2 pmol (∼25 ng) of *e*dsRNA was sufficient to induce complete hydrolysis of 20 fmol of CMV RNA 2 target in a standard slicer assay (not shown). Taken together, these data demonstrate that the *e*dsRNA constructs used are processed by DCLs under the conditions of the *in vitro* BYL system, such that the resulting siRNAs induce AGO/RISC-mediated hydrolysis of the original viral target RNA with efficiencies similar to those of the individual *e*siRNAs.

To determine the extent to which the DCL-processed siRNAs corresponded to the original *e*dsRNA-constituting *e*siRNAs, we performed the following experiment. In line with the scheme shown in Fig. 1A, the *e*dsRNAs dsCMV6-21 and dsCMV6-21o were exposed to the BYL-endogenous DCLs. After DCL-mediated processing, total RNA was extracted and small RNAs were sequenced using RNA-seq. Analysis of the size distribution of the siRNAs (Fig. 5A) showed almost identical patterns for the two dsRNA constructs. Due to the dominant activity of DCL3 in BYL, and in agreement with previous observations (Figs 1B and 4B), the predominant length of siRNA species processed from both *e*dsRNAs was 24 nt. However, in contrast to the previous data, the proportion of 21 nt siRNAs was significantly higher compared to 22 nt siRNAs (compare Figs 5A and 1B). The most interesting results were obtained when we quantified the guide and passenger strands of the *e*dsRNA-forming siR1172, siR1489, siR359, siR380, siR2041, siR1020, and the pseudo-siRNAs at the termini: this revealed a significant dominance of the read abundances of these same siRNAs compared to the total number of 21 nt reads (total number of 21 nt siRNAs generated) (Fig. 5B and Supplementary Fig. S7A). Approximately 60% of all 21 nt reads corresponded to the guide and passenger strands of the *e*dsRNA-constituent *e*siRNAs and pseudo-siRNAs, respectively (Table 3). In most cases, the guide strands were more readily measurable, and the detected amounts differed between the individual *e*siRNAs, which was explained by different protection against RNases, biases in the RNA-seq procedure, but also by the DCL activities on these *e*dsRNAs. Furthermore, the data obtained indicate that the DCL4 molecules present in BYL do indeed process the *e*dsRNAs predominantly in a phased manner, and that an *e*dsRNA consisting of a 21 nt pseudo-siRNA and *e*siRNA sequences produces predominantly 21 nt *e*siRNAs, as expected. However, DCL4 was not the only active DCL and, accordingly, other siRNA species were also produced from the *e*dsRNAs. Since the results with the blunt and 3′ overhang *e*dsRNAs were the same, we concluded that the nature of the *e*dsRNA termini has little effect on DCL-mediated processing in the plant extract (see 'Discussion').

The protective antiviral potential of *e*dsRNAs was evaluated in the next experiments of this study. To this end, we performed protection/infection experiments with *N. benthamiana* plants inoculated with 20 fmol of the three CMV genomic RNAs for a 'maximally successful challenge' and ∼70 pmol (8 μg) of dsCMV6-21o or dsCMV6-22o, respectively. As a control, we used a conventionally organized dsRNA, which we will refer to here as dsCMV (shown schematically in Fig. 4A; for sequence composition, see Supplementary Fig. S5).

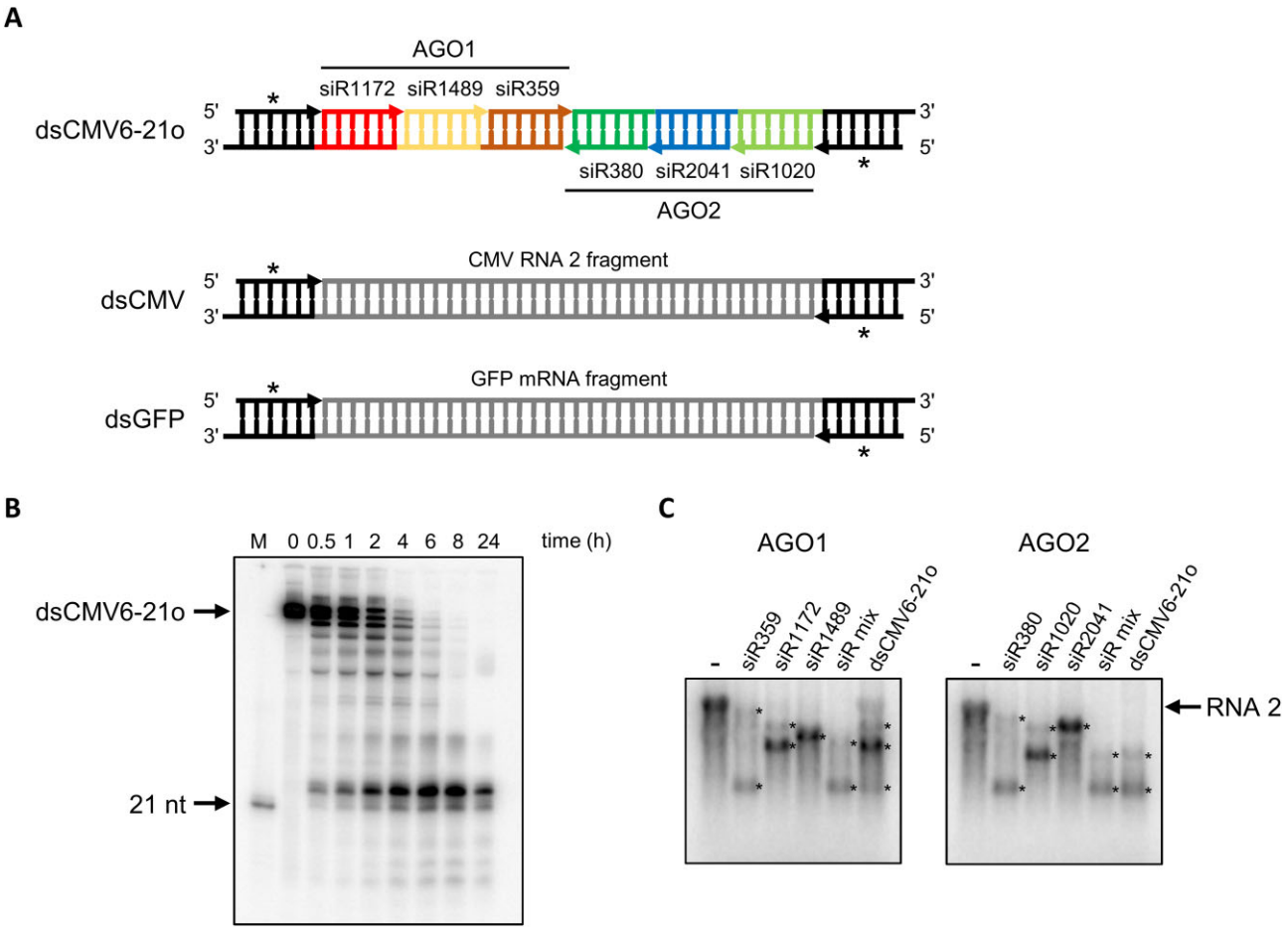

Figure 4. CMV *e*dsRNAs: composition, processing and *in vitro* silencing activity. (**A**) Exemplary *e*dsRNA and control dsRNAs. Top: Composition of an *e*dsRNA generated from two complementary RNA transcripts. The *e*dsRNA dsCMV6-21o contains a 21 nt long pseudo-siRNA at each end [symbolized by asterisks (*)] and six 21 nt long *e*siRNA sequences that have been shown to be effective against CMV RNA 2 *in vitro* and antivirally protective *in planta* (numbering according to Fig. 2 and Table 1). Guide strands (gs) are shown as arrows pointing in the 5′–3′ direction. The AGO1-specific gs are located on one RNA strand, the AGO2-specific gs are located on the other RNA strand. The example RNA shown here has 2 nt 3′ overhangs (dsCMV6-21o); however, *e*dsRNAs with blunt ends (dsCMV6-21) were also generated and tested. Middle: Control RNA dsCMV consists of pseudo-siRNA sequences at the ends and a 126 nt-long fragment of a ds version of CMV RNA 2 (corresponding to a length of six 21 nt-long siRNAs). By chance, the dsCMV also contains the sequences of two siRNAs that were identified as *e*siRNAs in the screen against CMV RNA 2. Bottom: Control RNA dsGFP consists of pseudo-siRNA sequences at the ends and a 126 nt long fragment of a ds version of GFP mRNA. The exact sequences of the dsRNAs shown are given in Supplementary Fig. S5. (**B**) Processing of an *e*dsRNA by DCLs *in vitro*. Labeled dsCMV6-21o was added to BYL and DCL-mediated processing analyzed over 24 h (see Supplementary Materials and methods) (M = 21 nt siRNA as marker). (**C**) Slicer assays with individual AGO1- and AGO2-specific *e*siRNAs from CMV RNA 2 and with the analogous *e*siRNAs generated from an *e*dsRNA in BYL. AGO1- or AGO2/RISC were reconstituted with individual *e*siRNAs, with an appropriate mix of these *e*siRNAs or with *e*siRNAs processed from the *e*dsRNA dsCMV6-21o in BYL by the DCLs present there. Endonucleolytic hydrolysis of labeled CMV RNA 2 target was detected by gel electrophoresis and autoradiography. Asterisks (*) indicate the generated cleavage products.

dsCMV consists of the previously described pseudo-siRNA sequences at the termini and a 126 nt-long continuous ds portion of CMV RNA 2 (corresponding to nucleotide positions 501–626 of CMV RNA 2 and a length of six 21 nt long siRNAs). Importantly, this ds segment of CMV RNA 2 contained the sequences of two siRNAs, siR557 and siR540, which were identified as *e*siRNAs in the previous screening procedure (see above and Supplementary Fig. S5). A ds segment of GFP mRNA, dsGFP, served as a negative control: as in all other cases, this dsRNA corresponded to a length of six siRNAs and contained pseudo-siRNA sequences at the termini. In addition, dsGFP contained the sequence of the siR gf698 control siRNA that was used previously (Supplementary Fig. S5). Fig. 6A shows representative images of plants treated as described, and Fig. 6B shows the overall course of several independent experiments performed with a representative number of plants and in which symptom development was monitored for 35 dpi.

Interestingly, treatment with dsCMV provided some protection and resulted in a delayed course of infection compared to negative controls in which plants were treated with dsGFP; however, no plants remained uninfected (without symptoms) at 35 dpi. The trend was significantly better for plants with dsCMV6-22o treatment with 20% remaining protected throughout the experiment. The most significant results were obtained when the plants were treated with dsCMV6-21o. In this case, 80%–100% of the plants remained protected against a CMV infection (Fig. 6 and Supplementary Fig. S7B). Importantly, comparable data were also obtained with plants monitored for 70 dpi, indicating that CMV infection was effectively controlled over longer periods of time and did not recur (Supplementary Fig. S8). Further control experiments

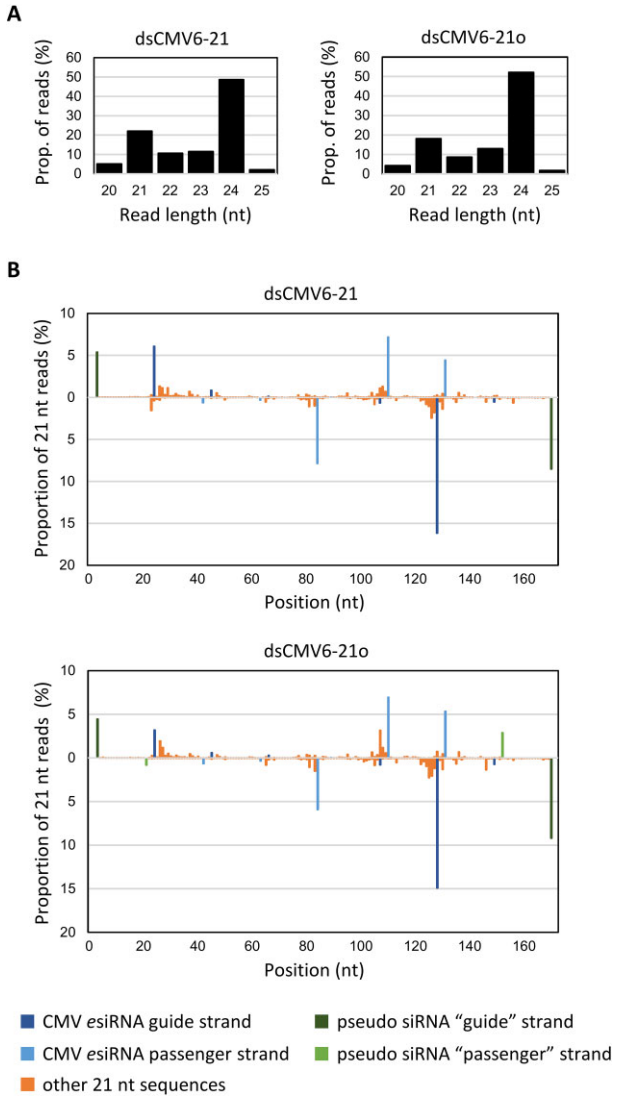

Figure 5. The *e*siRNA constituents are generated at high proportion from *e*dsRNA in BYL. dsCMV6-21 (blunt ends) and dsCMV6-21o (2 nt 3′ overhangs) were processed in BYL by the endogenous DCLs and the small RNA fraction analyzed by RNA-seq (see also scheme in Fig. 1A). (**A**) Size distribution of the 20–25 nt reads mapping to the *e*dsRNA sequences. (**B**) Proportion of guide and passenger strand reads among all 21 nt reads that mapped to the *e*dsRNA sequences; the peaks indicate the position of the 5′ nucleotide of reads with respect to the *e*dsRNA. Peaks corresponding to the pseudo-siRNA and *e*siRNA sequences are specifically colored. In the case of dsCMV6-21 there are no mapping 21 nt reads for the 'passenger' strands of the pseudo siRNAs, as the two 3′ nucleotides (position 20 and 21) are missing.

clearly excluded the possibility that the observed effects were caused by contamination of the dsRNA preparations with nonhybridized single-stranded components, which could theoretically hybridize with viral RNAs during inoculation and interfere with its translation or replication (Supplementary Fig. S7B).

Taken together, these data convincingly demonstrate the validity of our approach to develop efficient RNA actives against a devastating virus such as CMV. Our study identifies functional, highly efficacious antiviral *e*siRNAs in a first step and applies defined *e*dsRNAs consisting of these *e*siRNAs in a second step (Fig. 7).

Table 3. Proportion of CMV-specific *e*siRNA strands among all 21 nt siRNAs processed from two types of *e*dsRNAs in BYL

siRNA	dsCMV6-21		dsCMV6-21o	
	Guide strand (%)	Passenger strand (%)	Guide strand (%)	Passenger strand (%)
pseudo 1[a]	5.40	–	4.46	0.82
1172	6.09	0.65	3.19	0.66
1489	0.85	0.32	0.60	0.35
359	0.14	7.88	0.32	5.91
380	0.67	0.05	0.79	0.06
2041	16.18	7.18	14.91	6.96
1020	0.54	4.45	0.74	5.36
pseudo 2[a]	8.55	–	9.22	2.91
total	38.42	20.52	34.23	23.04

Discussion

RNA actives stimulate the silencing response and are of increasing interest for the control of plant pathogens and pests that destroy up to 30% of important staple crops each year and cause enormous economic loss [75, 28]. This holds true not only for viruses, but also for fungi, nematodes, and insects, where the RNA silencing machinery can be programmed to target their mRNAs. However, considerable optimization is required to obtain maximally effective RNA actives, as a significant number of siRNAs produced by DCLs from target RNAs have no antipathogenic effect. The use of siRNAs and dsRNAs, which can efficiently and multivalently induce silencing on an RNA target, therefore represents a significant improvement for both, HIGS as well as SIGS approaches. Transgenic expression would deliver the RNA agents to all organs of the plant, including the major sites of virus replication, and it would also allow RNA uptake by sap-sucking insects from the plant's phloem [76]. As mentioned, however, HIGS harbors a greater risk of resistance development; moreover, HIGS is not yet technically feasible for many plant species due to the lack of an established transformation protocol [28]. For SIGS and other topical applications requiring RNA to be taken up into plant cells, which is an ineffective process in itself [27], the use of effective RNA actives is all the more important.

The *e*NA screen procedure

Important steps towards effective RNA actives were the reconstitution of the cellular processes underlying RNA silencing *in vitro* and the application of this system to the empirical identification of *e*siRNAs that can mediate effective RISC-mediated slicing of target RNAs [33, 55, 56]. The current *e*NA screen procedure can already be carried out at a medium throughput level, i.e. several RNAs can be screened simultaneously and thus provide *e*siRNA candidates against various targets within a couple of weeks. The procedure, in particular the RNA-seq bottleneck, is currently being optimized for high throughput and should then also be usable in the form of a standard operating procedure.

Until now, use of the term 'effective siRNA' has been rather obscure. It evolved from *in silico* approaches that proposed RNA regions as siRNA targets because they encode conserved protein domains, or that attempted to predict RISC binding sites based on calculated RNA structures [77–79]. However, these predictions are associated with large uncertainties (reviewed in [80, 81]), as RNA structures are essentially functionally defined and can therefore only be verified by com-

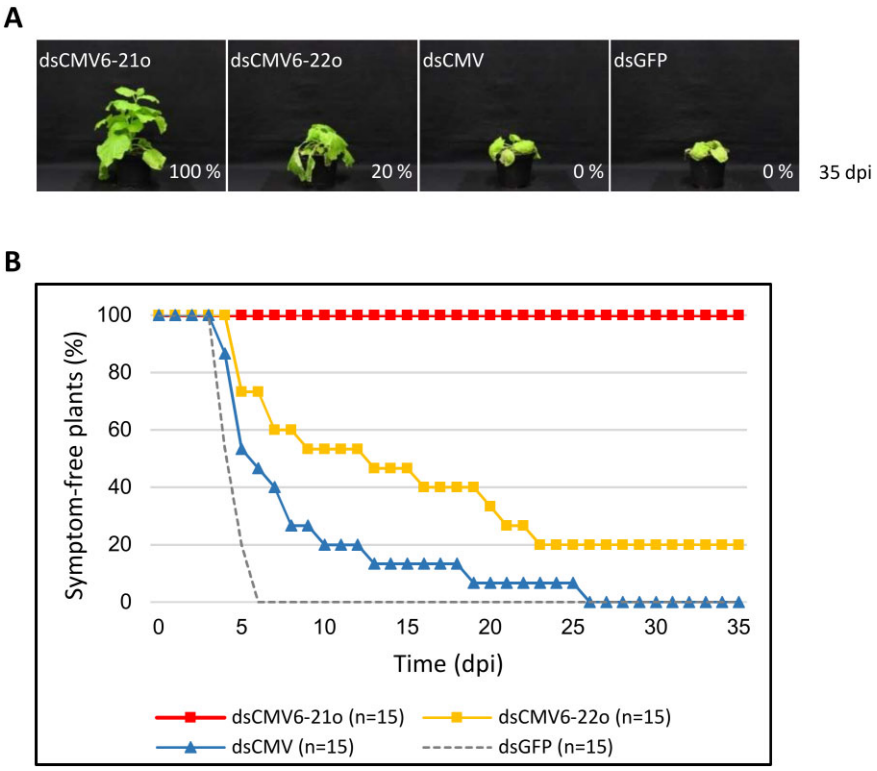

Figure 6. Comparison of the protective effect of different dsRNAs *in planta*. *N. benthamiana* plants were mechanically co-inoculated with different dsRNAs (see text) and with the genomic CMV RNAs 1, 2, and 3 and monitored for the appearance of CMV-specific symptoms for 35 dpi. Results are from two independent experiments; the total number of plants tested is indicated ($n = 15$). (**A**) Representative plant images 35 days after co-inoculation. The percentage of asymptomatic plants at 35 dpi is indicated for each dsRNA. (**B**) Percentage of asymptomatic plants over the entire course of the experiment.

plex empirical studies, usually in target cells or organisms [82, 83]. The *in vitro* system based on cytoplasmic extracts derived from plant cells, BYL, appears to be well-suited for this purpose. Our data suggest that target RNA folding variations under these conditions are similar to those in functional plant cells. During the *e*NA screen, identified *e*siRNAs could be simultaneously functionally characterized, namely by the affinity of their guide strands to the AGO protein used [12, 13] and by the successful interactions of the RISCs with a-sites of the target RNA [33–35]. In other words, the *e*siRNA candidates were determined by their activity, a reproducibly quantifiable AGO1- or AGO2/RISC-mediated hydrolysis of the respective target RNA *in vitro* (Fig. 2, Supplementary Fig. S1C, and Tables 1 and 2). Most importantly, as demonstrated here with the highly virulent CMV, most of the candidates actually showed a convincing protective effect when applied topically to plants, with certain *e*siRNAs reproducibly protecting 100% of individuals from infection (Fig. 3) [33]. It should be reiterated that the infections were carried out under an extremely strict regime. Using the mechanical 'rub-inoculation' method, 100% of the plants developed symptoms if left untreated. The fact that such a high level of protection against CMV was achieved under these conditions, which rarely or never occur in nature in this severity, illustrates the success of the *e*NA screening procedure (Figs 3 and 6).

In general, a correlation was found between slicing activity *in vitro* and the antiviral efficacy of the *e*siRNA candidates *in planta*. This was most evident for the *e*siRNAs identified against CMV RNA 2 and was previously observed in the characterization of *e*siRNAs against the CMV-unrelated TBSV [33]. This was less obvious for CMV RNA 3, as the number of identified *e*siRNA candidates, as well as their slicing activities and protective effects in plants were lower overall. As RNA 3 was generally inefficiently cleaved in the slicer assays, it can be assumed that the folding of this RNA generally results in poorer accessibility to RISC. The expression levels of the replicase proteins 1a and 2a are low in CMV-infected cells compared to those of the movement (3a) and capsid (3b) proteins [43]. RNA 3 therefore appears to be translated at a higher rate than RNA 2, making it also more difficult for RISC to access. In addition, in CMV-infected cells, RNA 3 (and its subgenomic RNA 4) was found to be more abundant than RNA 2 [50]. RNA 2 may therefore be a better target for RNA silencing, especially as the encoded RDR is the earliest protagonist of viral replication [84]. This idea is supported by the fact that the *e*siRNAs with the highest antiviral activity originate from the RNA 2-encoded 2a ORF. Interestingly, our *e*NA screens identified virtually no *e*siRNAs in the conserved terminal nontranslated regions of the viral RNAs (Fig. 2 and Supplementary Fig. S1B). These regions therefore appear to be particularly protected from RNA silencing, possibly due to their intense folding and functional activity in translation and replication [46, 85]. Taken together, our data reassert that the accessibility of functional RNA molecules to the silencing machinery can only be determined empirically.

Cross-protection by the identified *e*siRNAs

CMV isolates are classified into three major subgroups, including IA and II, which are found worldwide, and IB, which is primarily found in East Asia [43]. CMV Fny strain used in this study belongs to subgroup IA, and the *e*NA screens iden-

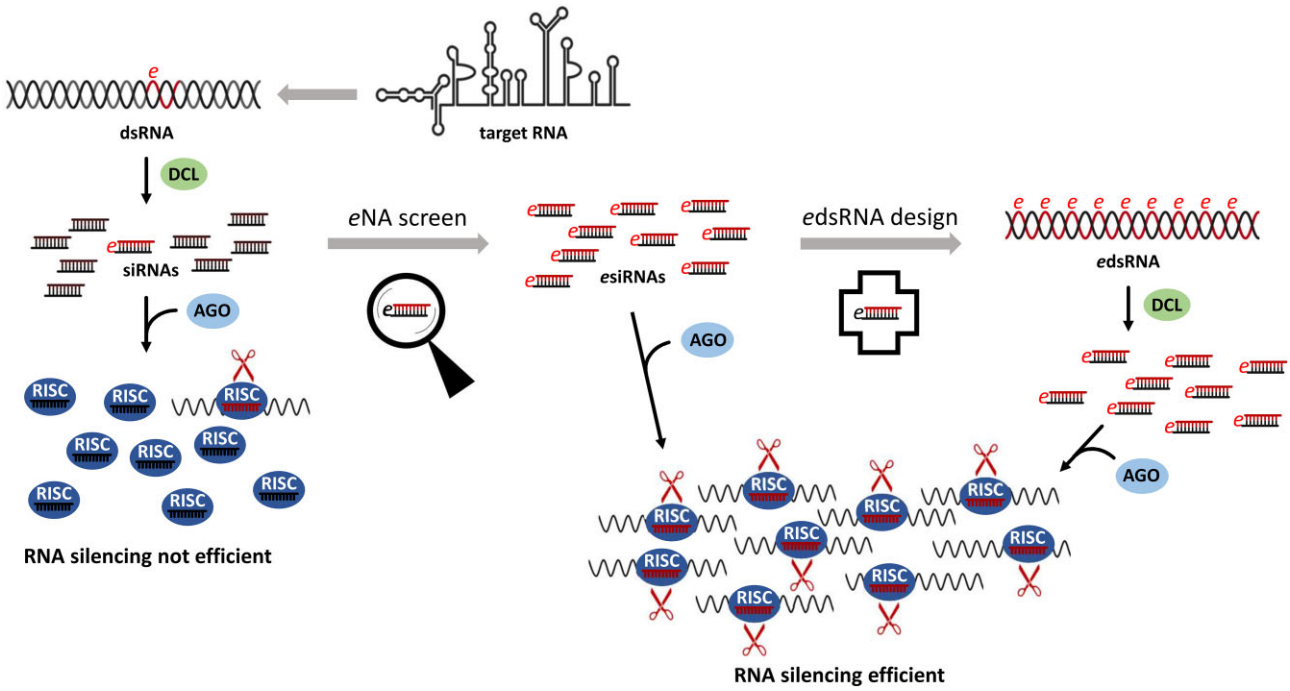

Figure 7. Identifying *e*siRNAs and designing *e*dsRNAs for significantly improved RNA-based crop protection. Upper/left parts: Upon infection of a plant with an RNA virus, viral dsRNA (e.g. replication intermediates) is detected by Dicer-like proteins (DCLs) and processed into a pool of siRNAs. The same happens with ds elements of other target RNAs and also with artificial dsRNAs generated from target RNAs. Of the produced siRNAs, only a few mediate efficient slicing of the target RNAs by AGO protein containing RISC resulting in inefficient RNA silencing. Middle/bottom parts: Functional siRNAs, *e*siRNAs, are characterized by a high affinity to antiviral AGO proteins and high accessibility of the respective complementary target sites in the target RNA. The *e*NA screen reliably identifies *e*siRNAs from siRNA pools, leading to an effective RNA silencing process. Right/bottom parts: The *e*siRNAs, which provide highly effective protection, e.g. against a viral infection, can be used to design *e*dsRNAs. The *e*dsRNAs are essentially composed of the sequences of the functionally characterized *e*siRNAs and are preferentially processed by the DCLs into these *e*siRNAs. Multivalent *e*dsRNAs thus have the potential to significantly increase the efficiency of RNA silencing-mediated protection of plants against pathogens such as RNA viruses.

tified *e*siRNAs capable of targeting very different regions of RNAs 2 and 3. Table 4 shows the sequence complementarity of the *e*siRNA candidates identified from CMV Fny to RNAs 2 or 3 of randomly selected strains of CMV subgroups IA (O, Y, Kor, I17F), IB (Rb, Nt9), and II (Trk7, LS), respectively. As anticipated, most homologies were found in the IA strains, less in the IB strains, and least of all in the II strains. It is known that the efficacy of RISC is reduced by one or more mismatches in the seed sequence, the primary interaction region of an siRNA or microRNA with the target RNA during the AGO/RISC-mediated silencing process [41], as well as by mismatches at the central positions 9–11 located opposite the cleavage site in the target RNA [86, 87]. On the other hand, it has been found in the plant system that microRNAs with a few mismatches in their 3′ region to a target RNA are often as effective in RNA silencing as miRs with full complementarity, which is probably also the case for siRNAs [86]. Taking all these factors into account, it is clear that most of the identified *e*siRNAs should be effective against many CMV strains of subgroups IA and IB and some also against subgroup II strains (Table 4). Thus, by using a combination of different *e*siRNAs targeting a-sites in different segments of the viral genome, broad-spectrum protection could be achieved, which is an important measure to counteract antigenic drifts or shifts of CMV (see also below).

Design of '*e*dsRNA actives'

For the optimal use of RNA actives in SIGS, HIGS, or other antipathogenic applications of RNA silencing, it is obvious that broad-spectrum protection against multiple variants of the pathogen can best be achieved in the form of applied multivalent '*e*dsRNAs' whose sequences are largely composed of multiple *e*siRNAs and which are processed by the plant's DCLs into these *e*siRNAs. Based on studies showing that dsRNAs longer than 130 nt induce RNA silencing up to 400-fold more strongly than 21 or 37 nt long dsRNAs [88], we here established *e*dsRNA molecules with a length of ca. 170 nt. These consisted of six *e*siRNA sequences and also had other important properties (Supplementary Fig. S5). The selection of *e*siRNAs to serve as *e*dsRNA building blocks was based on their functionality, i.e. their preferential incorporation into AGO1- or AGO2/RISC and their tested antiviral efficacy (Table 1). According to a model by Harvey *et al.* [89], the RNA-silencing defense of the plant against an infecting virus has several levels, with AGO1 being part of a first layer and AGO2 part of a second. In uninfected plants, the expression of AGO1 is usually higher than that of AGO2 [90], and there is evidence that miR403-loaded AGO1/RISC downregulate AGO2 mRNA expression post-transcriptionally [91]. In virus-infected *N. benthamiana*, an increase in AGO2 levels can be detected [92], and one model to explain this is that viral suppressors of RNA silencing, VSRs, sequester miR403 and thus override the suppression of AGO2 expression by AGO1 [58]. Consistent with this, VSRs such as the CMV 2b have been shown to bind small RNAs with high affinity and also directly inhibit AGO1 activity [93]. Thus, the activation of the second layer of the plant cell's RNA-silencing defense appears to be a direct consequence of the loss of the first layer [89]; when AGO1 activity is blocked, AGO2 is an important backup to

Table 4. Protection potential of the *e*siRNA candidates identified in this study with regard to the selected CMV strains O, Y, Kor, I17F, Rb, Nt9, Trk7, and LS from different subgroups

Subgroup IA							
O		Y		Kor		I17F	
RNA 2	RNA 3	RNA 2	RNA 3	RNA 2	RNA 3	RNA 2	RNA 3
149	35 (1)	149	35 **(3)**	149 **(2)**	35	149	35 (1)
186	151	186	151	186	151	186	151
359	239	359	239	359	239	359	239
380	358	380	358	380	358	380	358
407	478 (1)	407	478 (2)	407	478 (2)	407	478 **(1)**
449	496	449	496 **(1)**	449	496 (1)	449	496
540	507 **(1)**	540	507 (1)	540	507	540	507
557	592	557	592	557	592 **(1)**	557	592
1020	593	1020 (1)	593	1020 (2)	593 (1)	1020	593
1054 **(1)**	733	1054	733	1054	733	1054	733
1172	985	1172	985	1172	985	1172	985
1248	988	1248 **(1)**	988	1248	988	1248	988
1489	1019 **(1)**	1489	1019 (1)	1489	1019	1489 **(1)**	1019
1613 **(2)**	1098	1613	1098	1613	1098 (1)	1613	1098
1982	1394	1982	1394 **(1)**	1982	1394	1982	1394
2041 **(1)**	1569 **(1)**	2041	1569	2041	1569 **(1)**	2041	1569
2441		2441		2441		2441	
2562		2562		2562		2562	
2727		2727		2727 (1)		2727	

Subgroup IB				Subgroup II			
Rb		Nt9		Trk7		LS	
RNA 2	RNA 3	RNA 2	RNA 3	RNA 2	RNA 3	RNA 2	RNA 3
149 (1)	35	149 (1)	35	149 **(7)**	35 **(m)**	149 **(6)**	35 **(m)**
186	151	186 (2)	151	186 **(7)**	151 **(1)**	186 **(7)**	151 **(2)**
359	239	359	239 (1)	359 **(7)**	239 (1)	359 **(m)**	239 (1)
380	358	380 **(2)**	358 **(1)**	380 **(6)**	358 **(3)**	380 **(m)**	358 **(3)**
407	478 (1)	407 (1)	478 (2)	407 **(1)**	478 **(6)**	407 **(1)**	478 **(6)**
449	496 (1)	449 (1)	496 **(3)**	449 **(m)**	496 **(4)**	449 **(m)**	496 **(3)**
540	507 **(2)**	540	507 **(5)**	540 **(5)**	507 **(4)**	540 **(m)**	507 **(3)**
557	592	557	592	557 **(7)**	592 **(5)**	557 **(m)**	592 **(5)**
1020 (2)	593	1020 (1)	593	1020 **(7)**	593 **(5)**	1020 **(7)**	593 **(5)**
1054	733 **(1)**	1054 **(3)**	733 **(1)**	1054 **(7)**	733 **(4)**	1054 **(7)**	733 **(4)**
1172	985 **(1)**	1172 (1)	985 (3)	1172 **(4)**	985 **(m)**	1172 **(4)**	985 **(m)**
1248	988 (1)	1248 **(1)**	988 (2)	1248 **(m)**	988 **(m)**	1248 **(m)**	988 **(m)**
1489	1019	1489 **(2)**	1019	1489 **(7)**	1019 **(m)**	1489 **(7)**	1019 **(m)**
1613	1098	1613 **(2)**	1098 (1)	1613 **(8)**	1098 **(6)**	1613 **(8)**	1098 **(6)**
1982 (1)	1394	1982	1394 **(1)**	1982 **(4)**	1394 **(9)**	1982 **(4)**	1394 **(10)**
2041	1569	2041	1569 (3)	2041 **(2)**	1569 **(3)**	2041 **(2)**	1569 (1)
2441		2441 **(3)**		2441 **(m)**		2441 **(m)**	
2562		2562 (1)		2562 **(3)**		2562 **(2)**	
2727 (1)		2727 **(2)**		2727 **(3)**		2727 **(3)**	

(…) = number of mismatches between siRNA guide strand and target sequence
(**…**) = at least one of the mismatches affects the siRNA's seed sequence (nt 2–8) or central positions (nt 9–11)
(**m**) = multiple mismatches including insertions and/or deletions
Gray background = siRNA expected to mediate cleavage of the related target RNA with similar efficiency as the cleavage of the corresponding CMV Fny RNAs.

limit viral accumulation. The construction of *e*dsRNAs from AGO1- and AGO2-incorporating *e*siRNAs should therefore address both levels of the plant's antiviral RNAi immune response to achieve maximum antiviral efficacy.

The second important feature of the '*e*dsRNA active' toolkit established in this study concerned the 'pseudo-siRNA sequences' at the termini (Fig. 4A and Supplementary Fig. S5). On the DNA-level these sequences enabled high yield transcription. On the RNA-level, they were intended to support a phased processing by the DCLs by providing the appropriate distance between the 5′ ends of the dsRNA and the 5′ terminal siRNA sequence. Our data suggest that the pseudo-siRNA sequences do indeed serve both functions. In the *in vitro* system, we confirmed that the *e*dsRNAs are processed by the DCLs in such a way that large quantities of the individual *e*siRNAs are actually produced. For example, an *e*dsRNA with 21 nt pseudo-siRNA-termini generates large quantities of 21 nt *e*siRNAs, as predicted (Fig. 5B). We have also carried out experiments to test whether such processing of *e*dsRNA molecules also takes place in plants. For this purpose, leaves of *N. benthamiana* plants were inoculated in the same way as in the protection experiments (Fig. 6) and RNA-seq analysis was performed. Unsurprisingly, the *e*dsRNAs were found to be largely degraded into all forms of small RNA fragments by different RNase activities, which does not allow reliable conclusions to be drawn about the efficiency of DCL processing (Supplementary Fig. S9A). On the other hand, most *e*siRNA components could be detected, indicating DCL-mediated processing. This notion was particularly supported by the fact that the *e*siRNA siR2041, analogous to the *in vitro* DCL processing (Fig. 5 and Supplementary Fig. S7), was also most dominantly detectable *in planta* (Supplementary Fig. S9B).

The third feature of the '*e*dsRNA actives' developed here concerned optional 3′ overhangs. Interestingly, we observed no differences in antiviral activity when we used blunt or 3′ overhanging *e*dsRNAs in the *in vitro* and infectious virus-plant systems, respectively. This suggests that the DCLs involved in the processing of *e*dsRNAs to *e*siRNAs, namely DCL4 and/or DCL2, do not have substrate preferences that depend on the presence of 3′ overhangs.

The success of our approach—using such defined *e*dsRNA molecules consisting of functionally tested *e*siRNA components that most likely form the active ingredients of these *e*dsRNAs—was convincingly demonstrated in the plant protection experiments (Fig. 6): while a conventional dsRNA (dsCMV), which happened to contain two *e*siRNA sequences, only delayed the development of symptoms and thus the infection process without providing protection, the *e*dsRNAs had a significantly higher antiviral effect and completely protected 80%–100% of the infected plants. It is worth noting that this was also the case when the *N. benthamiana* plants were kept for 70 days, i.e. the clearance obtained was maintained throughout the life of the plant (Supplementary Fig. S8). The fact that in our experiments 21 nt long *e*siRNAs and *e*dsRNAs containing 21 nt *e*siRNA sequences were more efficient at antiviral RNA silencing than 22 nt *e*siRNAs and *e*dsRNAs containing 22 nt *e*siRNA sequences (Fig. 6 and Supplementary Fig. S4) can be explained by specificities of the CMV system (see Supplementary data for more details). Importantly at this point, however, we obtained no evidence that the 22 nt *e*siRNAs used in this study were able to enhance silencing by inducing secondary siRNA production.

The processing patterns of *e*dsRNAs in BYL and, as far as evaluable in plant, clearly showed that in addition to the expected *e*siRNAs, siRNAs of other lengths, in particular those with a length of 24 nt, are also produced (Fig. 5A). This is naturally due to the presence of other RNases, including DCL3. Another factor could be imperfect phase processing by DCL4 and/or DCL2. The production of unwanted siRNAs in plants is therefore not prevented by the use of *e*dsRNAs. However, it is clear that, compared to classically organized dsRNAs, the off-target effects of *e*dsRNA-generated siRNAs on mRNAs of the host plant [32, 39], as well as on nontarget organisms (NTOs) [42, 94], should be significantly reduced. One of the reasons for this is the large number and quantity of *e*siRNAs that are generated, as mentioned above. On the other hand, according to our data and the underlying principles of *e*NA screening, it can be assumed that *e*siRNAs are incorporated into RISC at considerably higher rates than other siRNAs generated from *e*dsRNAs due to their high affinity for AGO proteins. Furthermore, based on our observations, we believe that topical application requires significantly lower amounts of *e*dsRNA to achieve a protective effect than is the case with conventional dsRNAs. Accordingly, the use of *e*dsRNA actives in topical RNA silencing approaches will reduce the risk of decoy and off-target effects as well as the selection pressure for escape mutations. However, as with all applications of RNA actives, it will be crucial to proactively identify potential threats to NTOs through well-defined bioinformatic analyses of generated *e*dsRNA sequences.

General applicability of the study

Here, we have developed and applied *e*siRNA and *e*dsRNA actives against CMV. CMV is known to be one of the most highly variable plant pathogens. The success of our approach, *e*NA screen followed by *e*dsRNA design from the identified *e*siRNAs (Fig. 7), promises similar success for other plant pathogens, most of which have significantly less plasticity than CMV. *e*NA screen and *e*dsRNA design are easily transferable to mRNAs, and *e*dsRNAs, like other dsRNAs, can be produced in large quantities *in vitro*, in *Escherichia coli* or in other microorganisms [95–98]. The defined organization of *e*dsRNAs offers further advantages. For example, the number of *e*siRNA components can be significantly increased in order to enhance the multivalent activity against one or more RNA targets of a pathogen: A common standard for dsRNAs used are lengths of 200–1000 bp [23]. In this way, multiple traits with different modes of action can be attacked in one pathogen, a very important criterion for avoiding the development of resistances [28, 99].

It may also be possible to target different pathogens simultaneously. In this case, however, it is crucial to know the size of the siRNAs that are biologically active in the respective silencing systems of the targeted organisms. For example, in insects, 22 nt siRNAs are the most active in *Hymenoptera*/*Orthoptera*, 21 nt siRNAs in *Coleoptera* and *Diptera*, and 20 nt siRNAs in some *Lepidoptera* [100]. In addition, there appear to be differences in the recognition of RNA termini by the different Dicer proteins [74]. If there are uncertainties in this regard—indeed, these aspects are currently unknown for many plant pathogens—it will be possible to use differently structured *e*dsRNAs at the same time, e.g. with different termini and/or composed of *e*siRNAs of different lengths.

Overall, the results of this study significantly expand the potential for more efficient use of RNA in biological crop protection. It will now be important to further test and improve *e*siRNA and *e*dsRNA actives in combination with suitable formulations in agricultural applications, i.e. greenhouse or field trials.

Acknowledgements

We thank Gary Sawers for critical reading of the manuscript and Christine Hamann and Katja Rostowski for technical support. We thank the Leibniz Institute of Plant Biochemistry in Halle (Saale) and its gardeners for providing *N. benthamiana* plants. We are grateful to Prof. Fernando García-Arenal Rodríguez (Universidad Politécnica de Madrid) and Prof. John Carr (University of Cambridge) for providing the CMV Fny full-length cDNA clones.

Author contributions: Marie Knoblich (Investigation, Methodology, Validation), Torsten Gursinsky (Investigation, Methodology, Formal analysis, Data curation, Supervision, Validation, Conceptualization, Visualization, Writing—review and editing), Selma Gago-Zachert (Investigation, Methodology Formal analysis, Data curation, Supervision, Validation, Conceptualization, Writing—review and editing), Claus Weinholdt (Data curation, Formal analysis, Validation, Software), Jan Grau (Data curation, Formal analysis, Validation, Software, Resources, Conceptualization), and Sven-Erik Behrens (Conceptualization, Funding acquisition, Project administration, Resources, Supervision, Visualization, Writing—original draft, Writing—review and editing)

Supplementary data

Supplementary data is available at NAR online.

Conflict of interest

None declared.

Funding

This work was supported by a grant of the German Ministery of Education and Research, BMBF, IBÖM07: RNA PROTECT [FKZ 031B1008 and 031B1189], the German Science Foundation, DFG [grant number BE1885/15-1], and by the Investment Bank of Saxony-Anhalt [Fkz. ZS/2016/06/79 740 to M.K. and S.G.Z.].

Data availability

NGS datasets (raw reads) have been deposited in the European Nucleotide Archive (https://www.ebi.ac.uk/ena) under study accession number PRJEB76219.

References

1. Trebicki P. Climate change and plant virus epidemiology. *Virus Res* 2020;**286**:198059. https://doi.org/10.1016/j.virusres.2020.198059
2. Singh BK, Delgado-Baquerizo M, Egidi E *et al.* Climate change impacts on plant pathogens, food security and paths forward. *Nat Rev Micro* 2023;**21**:640–56. https://doi.org/10.1038/s41579-023-00900-7
3. Galvez LC, Banerjee J, Pinar H *et al.* Engineered plant virus resistance. *Plant Sci* 2014;**228**:11–25. https://doi.org/10.1016/j.plantsci.2014.07.006
4. Zvereva AS, Pooggin MM. Silencing and innate immunity in plant defense against viral and non-viral pathogens. *Viruses* 2012;**4**:2578–97. https://doi.org/10.3390/v4112578
5. Guo Z, Li Y, Ding S-W. Small RNA-based antimicrobial immunity. *Nat Rev Immunol* 2019;**19**:31–44. https://doi.org/10.1038/s41577-018-0071-x
6. Fukudome A, Fukuhara T. Plant dicer-like proteins: double-stranded RNA-cleaving enzymes for small RNA biogenesis. *J Plant Res* 2017;**130**:33–44. https://doi.org/10.1007/s10265-016-0877-1
7. Garcia-Ruiz H, Takeda A, Chapman EJ *et al. Arabidopsis* RNA-dependent RNA polymerases and dicer-like proteins in antiviral defense and small interfering RNA biogenesis during *Turnip Mosaic Virus* infection. *Plant Cell* 2010;**22**:481–96. https://doi.org/10.1105/tpc.109.073056
8. Qin C, Li B, Fan Y *et al.* Roles of dicer-like proteins 2 and 4 in intra- and intercellular antiviral silencing. *Plant Physiol* 2017;**174**:1067–81. https://doi.org/10.1104/pp.17.00475
9. Tang G, Reinhart BJ, Bartel DP *et al.* A biochemical framework for RNA silencing in plants. *Genes Dev* 2003;**17**:49–63. https://doi.org/10.1101/gad.1048103
10. Carbonell A, Carrington JC. Antiviral roles of plant ARGONAUTES. *Curr Opin Plant Biol* 2015;**27**:111–7. https://doi.org/10.1016/j.pbi.2015.06.013
11. Kobayashi H, Tomari Y. RISC assembly. Coordination between small RNAs and argonaute proteins. *Biochim Biophys Acta* 2016;**1859**:71–81.
12. Mi S, Cai T, Hu Y *et al.* Sorting of small RNAs into Arabidopsis argonaute complexes is directed by the 5' terminal nucleotide. *Cell* 2008;**133**:116–27. https://doi.org/10.1016/j.cell.2008.02.034
13. Takeda A, Iwasaki S, Watanabe T *et al.* The mechanism selecting the guide strand from small RNA duplexes is different among argonaute proteins. *Plant Cell Physiol* 2008;**49**:493–500. https://doi.org/10.1093/pcp/pcn043
14. Elbashir SM, Lendeckel W, Tuschl T. RNA interference is mediated by 21- and 22-nucleotide RNAs. *Genes Dev* 2001;**15**:188–200. https://doi.org/10.1101/gad.862301
15. Chen H-M, Chen L-T, Patel K *et al.* 22-Nucleotide RNAs trigger secondary siRNA biogenesis in plants. *Proc Natl Acad Sci USA* 2010;**107**:15269–74. https://doi.org/10.1073/pnas.1001738107
16. Wang X-B, Jovel J, Udomporn P *et al.* The 21-nucleotide, but not 22-nucleotide, viral secondary small interfering RNAs direct potent antiviral defense by two cooperative argonautes in *Arabidopsis thaliana*. *Plant Cell* 2011;**23**:1625–38. https://doi.org/10.1105/tpc.110.082305
17. Yoshikawa M, Han Y-W, Fujii H *et al.* Cooperative recruitment of RDR6 by SGS3 and SDE5 during small interfering RNA amplification in Arabidopsis. *Proc Natl Acad Sci USA* 2021;**118**:e2102885118. https://doi.org/10.1073/pnas.2102885118
18. Rosa C, Kuo Y-W, Wuriyanghan H *et al.* RNA interference mechanisms and applications in plant pathology. *Annu Rev Phytopathol* 2018;**56**:581–610. https://doi.org/10.1146/annurev-phyto-080417-050044
19. Zhao Y, Yang X, Zhou G *et al.* Engineering plant virus resistance: from RNA silencing to genome editing strategies. *Plant Biotechnol J* 2020;**18**:328–36. https://doi.org/10.1111/pbi.13278
20. Koch A, Wassenegger M. Host-induced gene silencing – mechanisms and applications. *New Phytol* 2021;**231**:54–9. https://doi.org/10.1111/nph.17364
21. Lassoued R, Phillips PWB, Smyth SJ *et al.* Estimating the cost of regulating genome edited crops: expert judgment and overconfidence. *GM Crops Food* 2019;**10**:44–62. https://doi.org/10.1080/21645698.2019.1612689

22. De Schutter K, Taning CNT, Van Daele L *et al.* RNAi-based biocontrol products: market status, regulatory aspects, and risk assessment. *Front Insect Sci* 2021;**1**:818037. https://doi.org/10.3389/finsc.2021.818037
23. Dalakouras A, Koidou V, Papadopoulou K. DsRNA-based pesticides: considerations for efficiency and risk assessment. *Chemosphere* 2024;**352**:141530. https://doi.org/10.1016/j.chemosphere.2024.141530
24. Pooggin MM. RNAi-mediated resistance to viruses: a critical assessment of methodologies. *Curr Opin Virol* 2017;**26**:28–35. https://doi.org/10.1016/j.coviro.2017.07.010
25. Rodrigues TB, Mishra SK, Sridharan K *et al.* First sprayable double-stranded RNA-based biopesticide product targets proteasome subunit beta type-5 in Colorado Potato Beetle (*Leptinotarsa decemlineata*). *Front Plant Sci* 2021;**12**:728652. https://doi.org/10.3389/fpls.2021.728652
26. Dalakouras A, Wassenegger M, Dadami E *et al.* Genetically modified organism-free RNA interference: exogenous application of RNA molecules in plants. *Plant Physiol* 2020;**182**:38–50. https://doi.org/10.1104/pp.19.00570
27. Bennett M, Deikman J, Hendrix B *et al.* Barriers to efficient foliar uptake of dsRNA and molecular barriers to dsRNA activity in plant cells. *Front Plant Sci* 2020;**11**:816. https://doi.org/10.3389/fpls.2020.00816
28. Beernink BM, Amanat N, Li VH *et al.* SIGS vs. HIGS: opportunities and challenges of RNAi pest and pathogen control strategies. *Can J Plant Pathol* 2024;**46**:675–89. https://doi.org/10.1080/07060661.2024.2392610
29. Le Page M. Gene-silencing spray lets us modify plants without changing DNA. *New Sci* 2017;3108.
30. Stokstad E. The perfect pesticide? *Science* 2024;**384**:1398–401. https://doi.org/10.1126/science.adr2991
31. Pantaleo V, Szittya G, Burgyán J. Molecular bases of viral RNA targeting by viral small interfering RNA-programmed RISC. *J Virol* 2007;**81**:3797–806. https://doi.org/10.1128/JVI.02383-06
32. Miozzi L, Gambino G, Burgyan J *et al.* Genome-wide identification of viral and host transcripts targeted by viral siRNAs in *Vitis vinifera*. *Mol Plant Pathol* 2013;**14**:30–43. https://doi.org/10.1111/j.1364-3703.2012.00828.x
33. Gago-Zachert S, Schuck J, Weinholdt C *et al.* Highly efficacious antiviral protection of plants by small interfering RNAs identified *in vitro*. *Nucleic Acids Res* 2019;**47**:9343–57. https://doi.org/10.1093/nar/gkz678
34. Brown KM, Chu C-Y, Rana TM. Target accessibility dictates the potency of human RISC. *Nat Struct Mol Biol* 2005;**12**:469–70. https://doi.org/10.1038/nsmb931
35. Ameres SL, Martinez J, Schroeder R. Molecular basis for target RNA recognition and cleavage by human RISC. *Cell* 2007;**130**:101–12. https://doi.org/10.1016/j.cell.2007.04.037
36. Gruber C, Gursinsky T, Gago-Zachert S *et al.* Effective antiviral application of antisense in plants by exploiting accessible sites in the target RNA. *Int J Mol Sci* 2023;**24**:17153. https://doi.org/10.3390/ijms242417153
37. Blevins T, Rajeswaran R, Aregger M *et al.* Massive production of small RNAs from a non-coding region of *Cauliflower mosaic virus* in plant defense and viral counter-defense. *Nucleic Acids Res* 2011;**39**:5003–14. https://doi.org/10.1093/nar/gkr119
38. Rajeswaran R, Golyaev V, Seguin J *et al.* Interactions of Rice tungro bacilliform pararetrovirus and its protein P4 with plant RNA-silencing machinery. *Mol Plant Microbe Interact* 2014;**27**:1370–8. https://doi.org/10.1094/MPMI-07-14-0201-R
39. Ramesh SV, Williams S, Kappagantu M *et al.* Transcriptome-wide identification of host genes targeted by tomato spotted wilt virus-derived small interfering RNAs. *Virus Res* 2017;**238**:13–23. https://doi.org/10.1016/j.virusres.2017.05.014
40. Leonetti P, Ghasemzadeh A, Consiglio A *et al.* Endogenous activated small interfering RNAs in virus-infected *Brassicaceae* crops show a common host gene-silencing pattern affecting photosynthesis and stress response. *New Phytol* 2021;**229**:1650–64. https://doi.org/10.1111/nph.16932
41. Jackson AL, Burchard J, Schelter J *et al.* Widespread siRNA "off-target" transcript silencing mediated by seed region sequence complementarity. *RNA* 2006;**12**:1179–87. https://doi.org/10.1261/rna.25706
42. Neumeier J, Meister G. siRNA specificity: rNAi mechanisms and strategies to reduce off-target effects. *Front Plant Sci* 2020;**11**:526455. https://doi.org/10.3389/fpls.2020.526455
43. Roossinck MJ. Evolutionary history of *Cucumber mosaic virus* deduced by phylogenetic analyses. *J Virol* 2002;**76**:3382–7. https://doi.org/10.1128/JVI.76.7.3382-3387.2002
44. Palukaitis P, García-Arenal F. Cucumoviruses. *Adv Virus Res* 2003;**62**:241–323. https://doi.org/10.1016/S0065-3527(03)62005-1
45. Jacquemond M. Cucumber mosaic virus. *Adv Virus Res* 2012;**84**:439–504. https://doi.org/10.1016/B978-0-12-394314-9.00013-0
46. Mochizuki T, Ohki ST. *Cucumber mosaic virus*: viral genes as virulence determinants. *Mol Plant Pathol* 2012;**13**:217–25. https://doi.org/10.1111/j.1364-3703.2011.00749.x
47. Morroni M, Thompson JR, Tepfer M. Twenty years of transgenic plants resistant to *Cucumber mosaic virus*. *Mol Plant Microbe Interact* 2008;**21**:675–84. https://doi.org/10.1094/MPMI-21-6-0675
48. Borah M, Berbati M, Reppa C *et al.* RNA-based vaccination of Bhut Jolokia pepper (*Capsicum chinense* Jacq.) against *Cucumber mosaic virus*. *Virusdisease* 2018;**29**:207–11.
49. Namgial T, Kaldis A, Chakraborty S *et al.* Topical application of double-stranded RNA molecules containing sequences of *Tomato leaf curl virus* and *Cucumber mosaic virus* confers protection against the cognate viruses. *Physiol Mol Plant Pathol* 2019;**108**:101432. https://doi.org/10.1016/j.pmpp.2019.101432
50. Holeva MC, Sklavounos A, Rajeswaran R *et al.* Topical application of double-stranded RNA targeting 2b and CP genes of *Cucumber mosaic virus* protects plants against local and systemic viral infection. *Plants* 2021;**10**:963. https://doi.org/10.3390/plants10050963
51. Routhu GK, Borah M, Siddappa S *et al.* Exogenous application of coat protein-specific dsRNA inhibits cognate *Cucumber mosaic virus* (CMV) of ghost pepper. *J Plant Dis Prot* 2022;**129**:293–300. https://doi.org/10.1007/s41348-021-00558-4
52. Komoda K, Naito S, Ishikawa M. Replication of plant RNA virus genomes in a cell-free extract of evacuolated plant protoplasts. *Proc Natl Acad Sci USA* 2004;**101**:1863–7. https://doi.org/10.1073/pnas.0307131101
53. Gursinsky T, Schulz B, Behrens S-E. Replication of *Tomato bushy stunt virus* RNA in a plant in vitro system. *Virology* 2009;**390**:250–60. https://doi.org/10.1016/j.virol.2009.05.009
54. Tschopp M-A, Iki T, Brosnan CA *et al.* A complex of Arabidopsis DRB proteins can impair dsRNA processing. *RNA* 2017;**23**:782–97. https://doi.org/10.1261/rna.059519.116
55. Iki T, Yoshikawa M, Nishikiori M *et al.* In vitro assembly of plant RNA-induced silencing complexes facilitated by molecular chaperone HSP90. *Mol Cell* 2010;**39**:282–91. https://doi.org/10.1016/j.molcel.2010.05.014
56. Schuck J, Gursinsky T, Pantaleo V *et al.* AGO/RISC-mediated antiviral RNA silencing in a plant *in vitro* system. *Nucleic Acids Res* 2013;**41**:5090–103. https://doi.org/10.1093/nar/gkt193
57. Gursinsky T, Pirovano W, Gambino G *et al.* Homeologs of the *Nicotiana benthamiana* antiviral ARGONAUTE1 show different susceptibilities to microRNA168-mediated control. *Plant Physiol* 2015;**168**:938–52. https://doi.org/10.1104/pp.15.00070
58. Pertermann R, Tamilarasan S, Gursinsky T *et al.* A viral suppressor modulates the plant immune response early in infection by regulating microRNA activity. *mBio* 2018;**9**:e00419-18. https://doi.org/10.1128/mBio.00419-18

59. Nagata T, Nemoto Y, Hasezawa S. Tobacco BY-2 cell line as the "HeLa" cell in the cell biology of higher plants. *Int Rev Cytol* 1992;**132**:1–30. https://doi.org/10.1016/S0074-7696(08)62452-3
60. Rizzo TM, Palukaitis P. Construction of full-length cDNA clones of *Cucumber mosaic virus* RNAs 1, 2 and 3: generation of infectious RNA transcripts. *Mol Gen Genet* 1990;**222**:249–56. https://doi.org/10.1007/BF00633825
61. Fátyol K, Ludman M, Burgyán J. Functional dissection of a plant Argonaute. *Nucleic Acids Res* 2016;**44**:1384–97. https://doi.org/10.1093/nar/gkv1371
62. Martin M. Cutadapt removes adapter sequences from high-throughput sequencing reads. *EMBnet j* 2011;**17**:10–2. https://doi.org/10.14806/ej.17.1.200
63. Langmead B, Trapnell C, Pop M *et al.* Ultrafast and memory-efficient alignment of short DNA sequences to the human genome. *Genome Biol* 2009;**10**:R25. https://doi.org/10.1186/gb-2009-10-3-r25
64. Edwards KD, Fernandez-Pozo N, Drake-Stowe K *et al.* A reference genome for *Nicotiana tabacum* enables map-based cloning of homeologous loci implicated in nitrogen utilization efficiency. *BMC Genomics* 2017;**18**:448. https://doi.org/10.1186/s12864-017-3791-6
65. Bombarely A, Rosli HG, Vrebalov J *et al.* A draft genome sequence of *Nicotiana benthamiana* to enhance molecular plant-microbe biology research. *Mol Plant Microbe Interact* 2012;**25**:1523–30. https://doi.org/10.1094/MPMI-06-12-0148-TA
66. Danecek P, Bonfield JK, Liddle J *et al.l.* Twelve years of SAMtools and BCFtools. *GigaScience* 2021;**10**:giab008. https://doi.org/10.1093/gigascience/giab008
67. Ho T, Wang H, Pallett D *et al.* Evidence for targeting common siRNA hotspots and GC preference by plant dicer-like proteins. *FEBS Lett* 2007;**581**:3267–72. https://doi.org/10.1016/j.febslet.2007.06.022
68. Sanan-Mishra N, Abdul Kader Jailani A, Mandal B *et al.* Secondary siRNAs in plants: biosynthesis, various functions, and applications in virology. *Front Plant Sci* 2021;**12**:610283. https://doi.org/10.3389/fpls.2021.610283
69. Dubrovina AS, Kiselev KV. Exogenous RNAs for gene regulation and plant resistance. *Int J Mol Sci* 2019;**20**:2282. https://doi.org/10.3390/ijms20092282
70. Nagano H, Fukudome A, Hiraguri A *et al.* Distinct substrate specificities of Arabidopsis DCL3 and DCL4. *Nucleic Acids Res* 2014;**42**:1845–56. https://doi.org/10.1093/nar/gkt1077
71. Wang Q, Xue Y, Zhang L *et al.* Mechanism of siRNA production by a plant dicer-RNA complex in dicing-competent conformation. *Science* 2021;**374**:1152–7. https://doi.org/10.1126/science.abl4546
72. Leonetti P, Consiglio A, Arendt D *et al.* Exogenous and endogenous dsRNAs perceived by plant dicer-like 4 protein in the RNAi-depleted cellular context. *Cell Mol Biol Lett* 2023;**28**:64. https://doi.org/10.1186/s11658-023-00469-2
73. Zhang H, Kolb FA, Brondani V *et al.* Human Dicer preferentially cleaves dsRNAs at their termini without a requirement for ATP. *EMBO J* 2002;**21**:5875–85. https://doi.org/10.1093/emboj/cdf582
74. Sinha NK, Iwasa J, Shen PS *et al.* Dicer uses distinct modules for recognizing dsRNA termini. *Science* 2018;**359**:329–34. https://doi.org/10.1126/science.aaq0921
75. Rizzo DM, Lichtveld M, Mazet JAK *et al.* Plant health and its effects on food safety and security in a one health framework: four case studies. *One Health Outlook* 2021;**3**:6. https://doi.org/10.1186/s42522-021-00038-7
76. Hunter WB, Wintermantel WM. Optimizing efficient RNAi-mediated control of hemipteran pests (psyllids, leafhoppers, whitefly): modified pyrimidines in dsRNA triggers. *Plants* 2021;**10**:1782https://doi.org/10.3390/plants10091782
77. Eastman P, Shi J, Ramsundar B *et al.* Solving the RNA design problem with reinforcement learning. *PLoS Comput Biol* 2018;**14**:e1006176. https://doi.org/10.1371/journal.pcbi.1006176
78. Lück S, Kreszies T, Strickert M *et al.* siRNA-Finder (si-Fi) software for RNAi-target design and off-target prediction. *Front Plant Sci* 2019;**10**:1023. https://doi.org/10.3389/fpls.2019.01023
79. Sciabola S, Xi H, Cruz D *et al.* PFRED: a computational platform for siRNA and antisense oligonucleotides design. *PLoS One* 2021;**16**:e0238753. https://doi.org/10.1371/journal.pone.0238753
80. Setten RL, Rossi JJ, Han S-P. The current state and future directions of RNAi-based therapeutics. *Nat Rev Drug Discov* 2019;**18**:421–46. https://doi.org/10.1038/s41573-019-0017-4
81. Crooke ST, Liang X-H, Baker BF *et al.* Antisense technology: a review. *J Biol Chem* 2021;**296**:100416. https://doi.org/10.1016/j.jbc.2021.100416
82. Zhang J, Fei Y, Sun L *et al.* Advances and opportunities in RNA structure experimental determination and computational modeling. *Nat Methods* 2022;**19**:1193–207. https://doi.org/10.1038/s41592-022-01623-y
83. Spitale RC, Incarnato D. Probing the dynamic RNA structurome and its functions. *Nat Rev Genet* 2023;**24**:178–96. https://doi.org/10.1038/s41576-022-00546-w
84. Seo J-K, Kwon S-J, Choi H-S *et al.* Evidence for alternate states of *Cucumber mosaic virus* replicase assembly in positive- and negative-strand RNA synthesis. *Virology* 2009;**383**:248–60. https://doi.org/10.1016/j.virol.2008.10.033
85. Barends S, Rudinger-Thirion J, Florentz C *et al.* tRNA-like structure regulates translation of brome mosaic virus RNA. *J Virol* 2004;**78**:4003–10. https://doi.org/10.1128/JVI.78.8.4003-4010.2004
86. Liu Q, Wang F, Axtell MJ. Analysis of complementarity requirements for plant microRNA targeting using a *Nicotiana benthamiana* quantitative transient assay. *Plant Cell* 2014;**26**:741–53. https://doi.org/10.1105/tpc.113.120972
87. Becker WR, Ober-Reynolds B, Jouravleva K *et al.* High-throughput analysis reveals rules for target RNA binding and cleavage by AGO2. *Mol Cell* 2019;**75**:741–55. https://doi.org/10.1016/j.molcel.2019.06.012
88. Kakiyama S, Tabara M, Nishibori Y *et al.* Long DCL4-substrate dsRNAs efficiently induce RNA interference in plant cells. *Sci Rep* 2019;**9**:6920. https://doi.org/10.1038/s41598-019-43443-9
89. Harvey JJW, Lewsey MG, Patel K *et al.* An antiviral defense role of AGO2 in plants. *PLoS One* 2011;**6**:e14639. https://doi.org/10.1371/journal.pone.0014639
90. Mallory A, Vaucheret H. Form, function, and regulation of ARGONAUTE proteins. *Plant Cell* 2010;**22**:3879–89. https://doi.org/10.1105/tpc.110.080671
91. Allen E, Xie Z, Gustafson AM *et al.* microRNA-directed phasing during trans-acting siRNA biogenesis in plants. *Cell* 2005;**121**:207–21. https://doi.org/10.1016/j.cell.2005.04.004
92. Várallyay É, Oláh E, Havelda Z. Independent parallel functions of p19 plant viral suppressor of RNA silencing required for effective suppressor activity. *Nucleic Acids Res* 2014;**42**:599–608. https://doi.org/10.1093/nar/gkt846
93. Csorba T, Kontra L, Burgyán J. Viral silencing suppressors: tools forged to fine-tune host-pathogen coexistence. *Virology* 2015;**479-480**:85–103. https://doi.org/10.1016/j.virol.2015.02.028
94. Chen J, Peng Y, Zhang H *et al.* Off-target effects of RNAi correlate with the mismatch rate between dsRNA and non-target mRNA. *RNA Biology* 2021;**18**:1747–59. https://doi.org/10.1080/15476286.2020.1868680
95. Tenllado F, Martínez-García B, Vargas M *et al.* Crude extracts of bacterially expressed dsRNA can be used to protect plants against virus infections. *BMC Biotechnol* 2003;**3**:3. https://doi.org/10.1186/1472-6750-3-3

96. Voloudakis AE, Holeva MC, Sarin LP *et al.* Efficient double-stranded RNA production methods for utilization in plant virus control. *Methods Mol Biol* 2015;**1236**:255–74. https://doi.org/10.1007/978-1-4939-1743-3_19
97. Niehl A, Soininen M, Poranen MM *et al.* Synthetic biology approach for plant protection using dsRNA. *Plant Biotechnol J* 2018;**16**:1679–87. https://doi.org/10.1111/pbi.12904
98. Hashiro S, Chikami Y, Kawaguchi H *et al.* Efficient production of long double-stranded RNAs applicable to agricultural pest control by *Corynebacterium glutamicum* equipped with coliphage T7-expression system. *Appl Microbiol Biotechnol* 2021;**105**:4987–5000. https://doi.org/10.1007/s00253-021-11324-9
99. Khajuria C, Ivashuta S, Wiggins E *et al.* Development and characterization of the first dsRNA-resistant insect population from western corn rootworm, *diabrotica virgifera virgifera* LeConte. *PLoS One* 2018;**13**:e0197059. https://doi.org/10.1371/journal.pone.0197059
100. Santos D, Mingels L, Vogel E *et al.* Generation of virus- and dsRNA-derived siRNAs with species-dependent length in insects. *Viruses* 2019;**11**:738. https://doi.org/10.3390/v11080738

Received: June 4, 2024. **Revised:** January 5, 2025. **Editorial Decision:** February 3, 2025. **Accepted:** March 3, 2025